UNIVERSIDADE DE SÃO PAULO
ESCOLA DE ENGENHARIA DE SÃO CARLOS

Kenny Anderson Queiroz Caldas

Controle Preditivo Baseado em Modelo de Veículo Autônomo para Direção Ecológica

São Carlos

2018

Kenny Anderson Queiroz Caldas

Model Predictive Eco-driving Control of Autonomous Vehicle

Dissertação apresentada à Escola de Engenharia de São Carlos da Universidade de São Paulo, para obtenção do título de Mestre em Ciências - Programa de Pós-Graduação em Engenharia Elétrica.

Área de concentração: Sistemas Dinâmicos

Orientador: Dr. Valdir Grassi Júnior

São Carlos

2018

Trata-se da versão corrigida da dissertação. A versão original se encontra disponível na EESC/USP que aloja o Programa de Pós-Graduação de Engenharia Elétrica.

Ficha catalográfica elaborada pela Biblioteca Prof. Dr. Sérgio Rodrigues Fontes da EESC/USP com os dados inseridos pelo(a) autor(a).

Caldas, Kenny Anderson Queiroz
C145c Controle Preditivo Baseado em Modelo de Veículo Autônomo para Direção Ecológica / Kenny Anderson Queiroz Caldas; orientador Valdir Grassi Júnior. São Carlos, 2018.

Dissertação (Mestrado) - Programa de Pós-Graduação em Engenharia Elétrica e Área de Concentração em Sistemas Dinâmicos -- Escola de Engenharia de São Carlos da Universidade de São Paulo, 2018.

1. Controle preditivo. 2. Veiculo autônomo. 3. Direção ecológica. 4. Economia de combustível. I. Título.

Eduardo Graziosi Silva - CRB - 8/8907

FOLHA DE JULGAMENTO

Candidato: Engenheiro **KENNY ANDERSON QUEIROZ CALDAS.**

Título da dissertação: "Controle preditivo baseado em modelo de veículo autônomo para direção ecológica".

Data da defesa: 26/02/2018.

Comissão Julgadora: **Resultado:**

Prof. Doutor **Valdir Grassi Junior** Aprovado
(Orientador)
(Escola de Engenharia de São Carlos/EESC)

Prof. Associado **Adriano Almeida Gonçalves Siqueira** Aprovado
(Escola de Engenharia de São Carlos/EESC)

Prof. Dr. **Guilherme Vianna Raffo** Aprovado
(Universidade Federal de Minas Gerais/UFMG)

Coordenador do Programa de Pós-Graduação em Engenharia Elétrica:
Prof. Associado **Luis Fernando Costa Alberto**

Presidente da Comissão de Pós-Graduação:
Prof. Associado **Luis Fernando Costa Alberto**

ACKNOWLEDGEMENTS

I would like to thank my supervisor, Professor Valdir Grassi Junior, for accepting me as his masters student and for all support, suggestions and trust given during these two years. It was a wonderful experience to work in such an interesting project. I also would like to thank the São Carlos School of Engineering, University of São Paulo, the department of Electrical Engineering for the resources provided during the development of the project and FDTE for the financial aid.

I would like to thank to all friends I made at the university, in special to everyone at LASI, for sharing many good moments with me. I'm grateful to everyone at LRM for the support given during the tests required for the development of this thesis. I also want to thank all the professors that helped me during this time.

I'm very grateful to my family for always helping me to pursue my dreams, believing in me in every new journey I start in my life. I would like to thank in special to my fiancee Fabiana, for staying by my side in all this time, for the patience, caring and love, giving me the strength to overcome all challenges.

ABSTRACT

CALDAS, K. A. Q. **Model Predictive Eco-driving Control of Autonomous Vehicle**. 2018. 68p. Thesis (Masters) - São Carlos School of Engineering, University of São Paulo, São Carlos, 2018.

The purpose of this masters thesis is the implementation of a model-based predictive controller for eco-driving in autonomous ground vehicles. Eco-driving consists of a group of strategies adopted by a driver aiming to reduce fuel consumption and improvement of safety and comfort levels during a trip. Through the use of digital maps and a GPS module, the predictive controller can calculate a sequence of control input to smooth the vehicle's acceleration and braking along the route in critical parts, such as uphills, downhills and curves, following the speed limits of each road. This is accomplished by predictions based on the mathematical model of the vehicle and estimation of gasoline expenditure. The chosen optimizer algorithm is called C/GMRES, where its main advantage from the traditional methods is that the solution of the optimal problem does not required iterative searches, which greatly reduces the computational burden, allowing a real time implementation. The proposed control strategy was implemented in two routes, in a city and highway scenarios, in a simulated environment. The obtained results were considered satisfactory and showed the predictive controller potential to deal with the fuel consumption problem in autonomous vehicles.

Keywords: Predictive control. Autonomous vehicle. Ecological driving. Fuel economy.

RESUMO

CALDAS, K. A. Q. **Controle Preditivo Baseado em Modelo de Veículo Autônomo para Direção Ecológica**. 2018. 68p. Dissertação (Mestrado) - Escola de Engenharia de São Carlos, Universidade de São Paulo, São Carlos, 2018.

A proposta desta dissertação de mestrado é a implementação de um controlador preditivo baseado em modelo para direção ecológica em veículos autônomos terrestres. Direção ecológia consiste em um conjunto de estratégias que um motorista pode adotar visando a redução do consumo de combustível e melhora dos níveis de segurança e conforto durante uma viagem. Através da utilização de mapas digitais e de um módulo de GPS, o controlador preditivo pode calcular uma sequência de entradas de controle visando suavizar a aceleração e frenagem do veículo ao longo do percurso em trechos críticos como ladeiras, declives e em curvas, respeitando o limite de velocidade de cada estrada. Isto é realizado por meio de predições baseadas no modelo matemático do veículo e da estimação do gasto de gasolina. O algoritmo de otimização utilizado é chamado de C/GMRES, onde a sua principal vantagem em relação aos métodos tradicionais consiste na solução do problema de otimização não necessitar de buscas iterativas, o que reduz consideravelmente o custo computacional de processamento, permitindo a sua implementação em tempo real. A estratégia de controle proposta foi implementada em dois percursos, em trecho urbano e rodoviário, em um ambiente simulado no MATLAB. Os resultados obtidos foram considerados satisfatórios e demonstraram o potencial que o controlador preditivo possui para o problema da redução do consumo de combustível em veículos autônomos.

Palavras-chave: Controle preditivo. Veiculo autônomo. Direção ecológica. Economia de combustível.

LIST OF FIGURES

LIST OF TABLES

LIST OF ABBREVIATIONS AND ACRONYMS

MPC	Model Predictive Control
GPS	Global Positioning System
USA	United States of America
DARPA	Defense Advanced Research Projects Agency
IMU	Inertial Measurement Unit
LIDAR	Light Detection And Ranging
ABS	Anti-lock Breaking System
PI	Proportional Integral
PID	Proportional Integral Derivative
LQR	Linear Quadratic Regulator
VT-CPFM-2	Virginia Tech Comprehensive Power-based Fuel Consumption Model 2
EPA	Environmental Protection Agency
ROS	Robot Operating System
CAN	Controller Area Network
LRM	Mobile Robot Laboratory
GMRES	Generalized Minimal Residual Method
C/GMRES	Continuation Generalized Minimal Residual Method
NMPC	Nonlinear Model Predictive Control
EV	Electrical Vehicle
EDC	Eco-driving Controller
FSC	Fixed Speed Controller
USP	Universidade de São Paulo
RTK	Reak Time Kinematic

LIST OF SYMBOLS

x	State vector
u	Control input
p	Time-varying parameter
φ	Penalty function
$f(x, u)$	State equation
t	Current time
T	Prediction horizon length
J	Cost function
L	Stage cost function
$u*$	Optimal control input
s	Distance travelled
a	Acceleration
f_{curv}	Curvature function
R_{curv}	Curve radius
a_{lat}	Lateral acceleration
ω_e	Engine speed
ω_{idle}	Engine speed at idle
ω_{red}	Redline engine speed
ξ_i	ith Gear ratio
r	Wheel radius
P	Vehicle power
β_i	ith VT-CPFM-2 constant
P_{mfo}	Idling fuel mean pressure
d	Engine displacement

Q	Fuel lower heating value
N_{cil}	Number of engine cylinders
F_{city}	Fuel consumed for the EPA city drive cycle
F_{hwy}	Fuel consumed for the EPA highway drive cycle
FE_{city}	Estimated fuel consumption for a city route
FE_{hwy}	Estimated fuel consumption for a highway route
F_{hwy}	Fuel consumed for the EPA highway drive cycle
T_{city}	Duration of the EPA city cycle
T_{hwy}	Duration of the EPA city cycle
P_{city}	Power exerted for the EPA city drive cycle
P_{hwy}	Power exerted for the EPA highway drive cycle
ω_{city}	Engine speed for the EPA city drive cycle
ω_{hwy}	Engine speed for the EPA highway drive cycle
v	Vehicle velocity
M	Vehicle mass
F_T	Vehicle traction force
F_{roll}	Vehicle rolling resistance force
F_{grav}	Vehicle gravitational resistance force
F_{drag}	Vehicle aerodynamic drag force
g	Gravitational acceleration
μ	Lagrange multiplier
C_D	Drag coefficient
ρ	Air density
A_f	Frontal area of the vehicle
θ	Road slope angle
u_{min}	Lower control input limit

u_{max}	Upper control input limit
M_{ta}	Propulsive axle mass
C	Control input constraint
γ	Road adhesion coefficient
w_i	Cost function ith weighting constant
a_{latMax}	Maximum lateral acceleration
a_{max}	Maximum longitudinal acceleration
v_{lim}	Velocity limit
R_{alt}	Road altitude
η_d	Engine efficiency
v_{Ref}	Desired vehicle velocity
H	Hamiltonian function
λ	Costate
k	Current iteration
N	Number of prediction steps
n	Iteration multiplier
h	Prediction step size
$kmax$	C/GMRES iteration number
u_{slk}	Slack control input

CONTENTS

1 INTRODUCTION

The transportation sector currently corresponds for approximately 25% of world energy consumption and CO_2 emissions, taking into account that much of the energy source comes from fossil fuels. Therefore, it not only increases the concern about the environmental impact of producing polluting gases, but also raises the cost of oil barrels (SCHMITT, 2010). There are many aspects that can affect the energy consumption of a vehicle such as weather phenomenons, road surface conditions, driver's behavior, selected driving gear and physical characteristics of the vehicle (KAMAL et al., 2013), (VAEZIPOUR; RAKOTONIRAINY; HAWORTH, 2015). To address these problems, the strategies used on eco-driving have been receiving great attention recently.

Eco-driving is a concept aimed at reducing fuel consumption based on a group of behaviors that can be adopted by the driver. A few of strategies used are driving at an even pace, accelerating and braking smoothly, using the correct gears for each situation and maintaining a constant speed. A study conducted in Australia in 2015 by Jeffreys, Graves & Roth (2016) showed that drivers who received a training and adopted eco-driving have been able to reduce 4.6%, or 0.51 liters on a 100-kilometer course, compared to those who did not, which would result in 169 kilograms less CO_2 in the atmosphere over a year. Another study, conducted by Barth & Boriboonsomsin (2009), consisting of a system of real-time recommendations for drivers, has been able to save up to 20% of fuel and a significant reduction in emissions of polluting gases. It is also important to note that the advantages of eco-driving go beyond fuel saving and CO_2 reduction, since it allows to cause fewer accidents and decrease traffic fatalities (BARKENBUS, 2010).

Through the new technologies involving autonomous vehicles, it has been possible to see the decision-making capability shifting from the human driver to the vehicle (MERSKY; SAMARAS, 2016). There are many companies currently investing in self-driving cars, such as Apple, Google, Mercedes-Benz, BMW, Volvo and Uber, to name a few. The Tesla Motors' Model S vehicle is already available on the market, enabling auto steering, lane changing and parking features for the driver (INSIGHTS, 2016). The processing power existent in autonomous vehicles would allow the implementation of strategies used on eco-driving in a more efficient way, since it could analyze the information obtained from its environment and current state to obtain the best action to take.

One of the main control techniques implemented in this case is model-based predictive control (MPC), also known as receding horizon control. According to Grüne & Pannek (2011), the main idea of a predictive controller, linear or nonlinear, is to use the model of a process to predict and optimize its future behavior. In other words, the MPC strategy is executed in close-loop, where an open loop optimal control problem is

solved within a fixed prediction horizon to obtain a sequence of optimal control inputs. Only the first element of this sequence is used and the remaining entries are discarted. The prediction horizon window is shifted to the next step and the process is repeated (ALLGÖWER; FINDEISEN; NAGY, 2004).

The application of a MPC controller involving autonomous vehicle extends to many fields of study, such as trajectory tracking (FALCONE et al., 2007), (FALCONE et al., 2008), (KIM; KIM; SUNWOO, 2014), (RAFFO et al., 2009), collision avoidance (YOON et al., 2009), (JI et al., 2017) and the main objective of this project, fuel economy.

The current master project seeks to implement a longitudinal model-based predictive eco-driving control of an autonomous vehicle, in order to reduce its fuel consumption. The driver's comfort is also considered in this work. Therefore, the autonomous vehicle will consider the strategies covered in eco-driving to adjusts its acceleration and braking levels according to the physical characteristic of the route.

The controller uses the information from the digital map of the route such as longitude and latitude, to calculate the curvature and slope profile of the road. Thus, the autonomous vehicle increases its velocity before entering an uphill section and decelerate using engine braking whenever possible. This improves the vehicle's fuel economy by reducing the tractive power required to maintain the desired velocity. The influence of the lateral acceleration existing on the vehicle during steering is also considered for comfort reasons, therefore, the controller prioritizes the driver's comfort during curves by reducing the vehicle's velocity. At last, the specific speed limits of each section of the route is also considered, to ensure the vehicle operate under the maximum allowed speed.

The remainder of the thesis is organized as follows: Chapter 2 gives a brief definition of autonomous vehicle and its early development, an overview of the model-based predictive control strategy and the main concepts of eco-driving. Chapter 2 also reviews the state of the art related to fuel economy studies in ground vehicles, the implementation of MPC in autonomous vehicles and the how this thesis differs from recent works. Chapter 3 details the vehicle's mathematical models used in the project and in Chapter 4 is covered the conditions and steps required for the MPC strategy implementation. The results obtained through simulations of the proposed MPC controller is compared with a different controller in Chapter 5 to evaluate its performance. The concluding remarks of this thesis and ideas for future work are presented in Chapter 6.

2 BIBLIOGRAPHIC REVIEW

This chapter will cover the main theoretical concepts used in this project. The definition of autonomous vehicles and their main characteristics will be introduced, the main parameters and their importance in model predictive control and the concept of ecological driving and factors that can affect the fuel consumption.

2.1 Autonomous vehicles

A vehicle can be defined autonomous when it can make decisions and drive without human intervention (OZGUNER; ACARMAN; REDMILL, 2011). Although the beginning of studies in autonomous driving does not have an unanimity starting point, since different papers refers to Japan (AHSAN; ALIMGEER, 2013) or USA (LUETTEL; HIMMELSBACH; WUENSCHE, 2012), the turning point for the development of autonomous vehicles was during the Defense Advanced Research Projects Agency (DARPA) Grand Challenge in 2004 (JO et al., 2014), (OZGUNER; ACARMAN; REDMILL, 2011).

DARPA conducted an event where a car should travel through an off-road course from Los Angeles to Las Vegas, in which the winner should finish in less than 10 hours, without human intervention. A prize of $ 1 million dollars would be given for the team that could complete the designed course (OZGUNER; ACARMAN; REDMILL, 2011), but in this first challenge there was no winner. DARPA also promoted two more events. In 2005 the winning team was from the Stanforf University headed by Sebastian Thrun. The third race was taken in 2007 and it was know as DARPA Urban Challenge, because the course involved an urban area in which dynamic traffic and signaling would be considered. Tartan Racing, by Carnegie Mellon University with cooperation of General Motors Corporation, won in this year. These challenges pushed the development of new technologies, such as drive-by-wire steering, throttle and brake control. Many sensors were also developed or improved, including Light Detection and Ranging (LIDAR) sensor, radars, Global Positioning System (GPS), Inertial Measurement Unit (IMU) and cameras (OZGUNER; ACARMAN; REDMILL, 2011).

The technologies present in autonomous vehicles covers a variety of features, such as cruise control, Antilock Brake System (ABS), lane departure avoidance, obstacle avoidance, car following and so on. An illustration of a generic autonomous vehicle can be seen on Figure 1. The functions that an autonomous vehicle should perform during a travel are (OZGUNER; ACARMAN; REDMILL, 2011):

- Self-sensing its current speed and acceleration.

- Locate itself in an absolute coordinate system, by using a GPS or a map database.
- Sensing environmental objects, such as lane markings, traffic signaling, obstacles, other vehicles and so on.
- Control the vehicle's actuators based on the desired task.

Figure 1: Generic illustration of an autonomous vehicle.

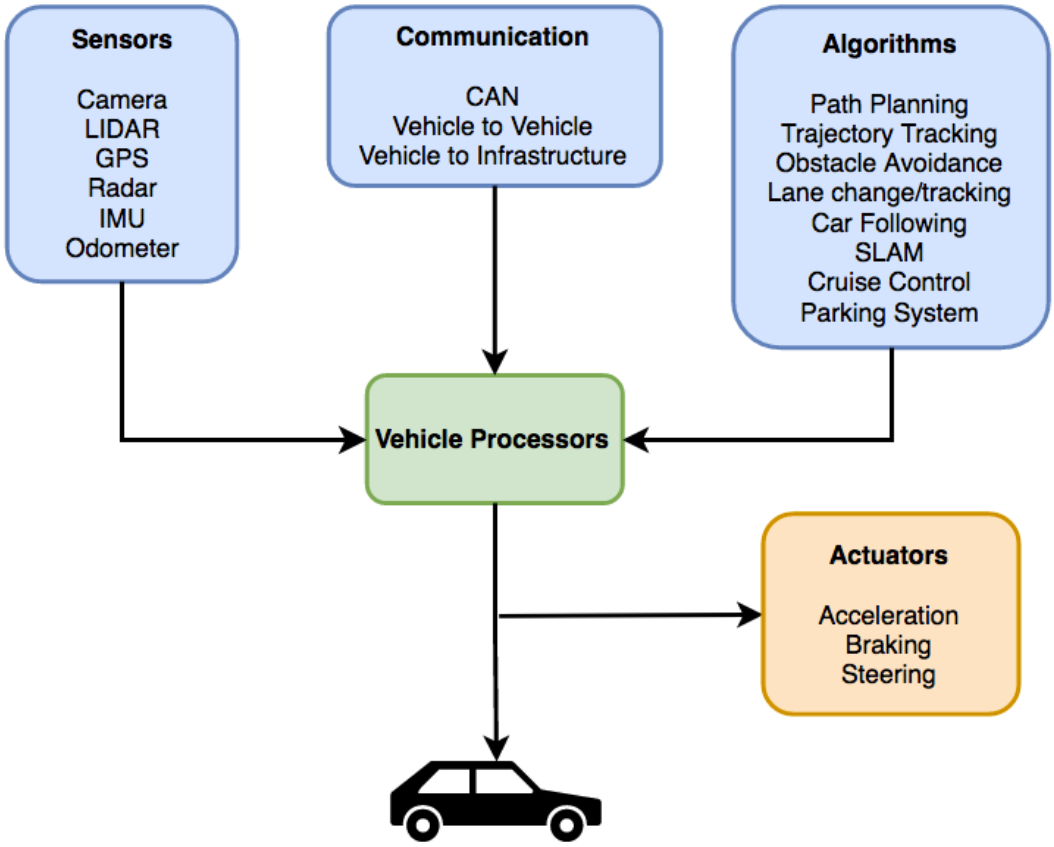

Source: Author.

The decision-make potential of autonomous vehicles can bring many advantages to vehicular traffic. For example, it could increase the traffic flow speed, consume less fuel and reduce the pollution, avoid accidents and make faster trips (AHSAN; ALIMGEER, 2013).

2.2 Model predictive control

The term Model Predictive Control (MPC), also know as Receding Horizon Control (RHC), unlike other control techniques such as PID and LQR does not specify to a particular control strategy, but covers a great variety of control methods. The basic structure of the MPC strategy is shown on Figure 2.

Figure 2: Block diagram of the MPC strategy.

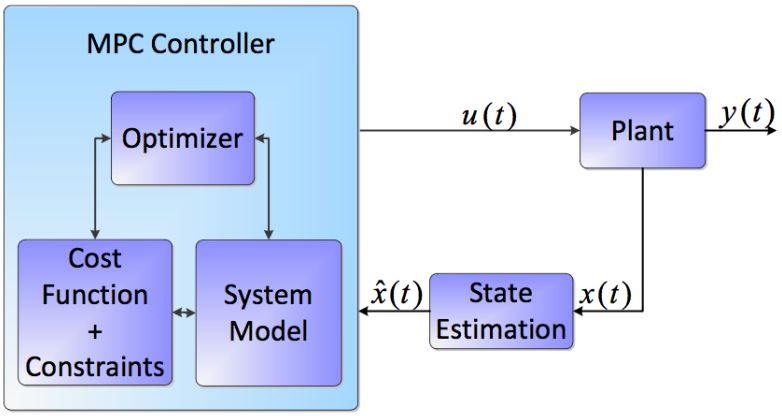

Source: Abbas (2011)

2.2.1 System model

A general nonlinear model of a system can be represented by Equation (2.1), where $x(t)$, $u(t)$ and $p(t)$ denotes the state vector, the input vector and time-dependent parameters (OHTSUKA, 2004).

$$\dot{x}(t) = f(x(t), u(t), p(t)) \tag{2.1}$$

The mathematical model of a system is the most important part of the MPC, since it will permit the controller to predict the future behavior of the system. In order to do this, the model needs to be able to represent the relation of the output and input variables (CAMACHO; BORDONS, 1999), (ROSSITER, 2003).

2.2.2 Cost function

To find the optimal control input sequence for the future states of the system, at each time t the MPC minimizes a performance index until time $t + T$, where T represents the control horizon length. A general form for the performance index is

$$J = \varphi(x^u(t+T; t, x(t)), p(t+T) + \int_t^{t+T} L(x^u(t'; t, x(t)), u(t'), p(t'))dt', \tag{2.2}$$

where $x^u(t'; t, x(t))$ represents the state trajectory with input u, starting from $x(t)$ at time t, $\varphi(x^u(t+T; t, x(t))$ is the terminal cost function, $p(t+T)$ are time-varying parameters and L the stage cost.

The terminal cost is one of the first proposals to modify the performance index in order to ensure closed-loop stability. It will make a finite-horizon MPC behave as an infinite-horizon MPC. However it needs to meet certain criteria to be used correctly in an optimization problem (MAYNE et al., 2000).

The cost function, also known as objective function, is the criteria that the MPC will use to judge which control action will be the best for each future step of the state trajectory. The lower the numerical value of the cost function is at each step, the better the control action will be at that instant.

2.2.3 Receding horizon strategy

The MPC can generate an optimal sequence of control inputs from time t to $t+T$, based on the measured state $x(t)$. Instead of using the entire sequence on the system for the next n steps, only the first element $u^*(0)$ is used and the whole process is repeated again. This is called the moving horizon, or receding horizon strategy (CAMACHO; BORDONS, 1999), (ROSSITER, 2003). An illustration of this process can be seen on Figure 3.

Figure 3: Illustration of the moving horizon strategy.

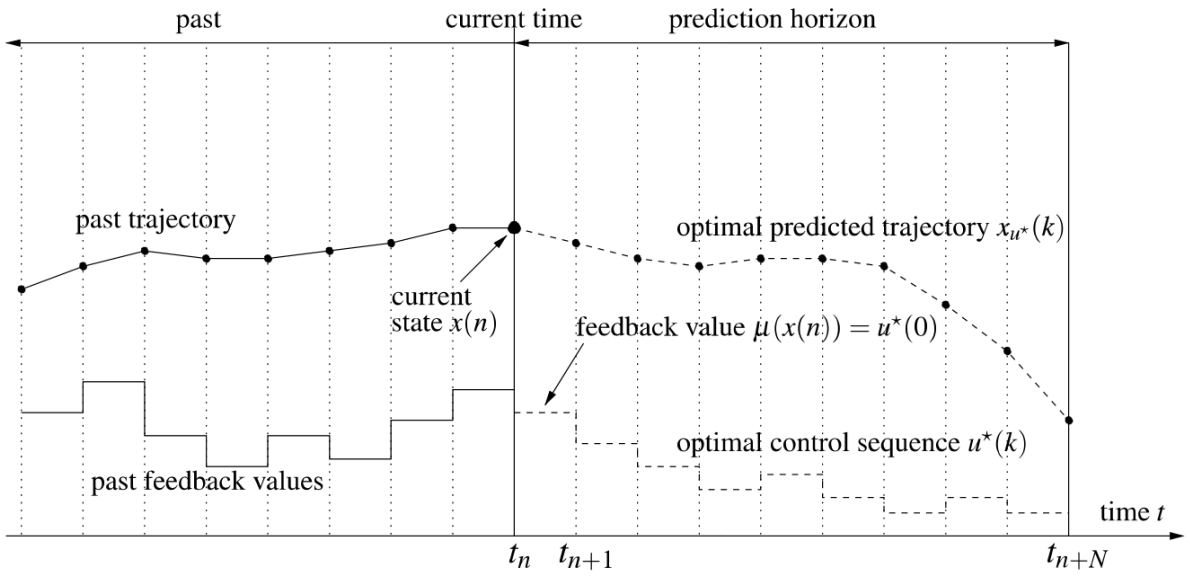

Source: Grüne & Pannek (2011).

The moving horizon strategy is used to provide robustness implicitly on the system model. Since it is very difficult to have a precise mathematical description of a real world process, there are disturbances that can deviate the predicted future outputs from the measured outputs. By updating the control sequence at each time step t, the MPC will be able to compare the system current behavior with the predicted model obtained from equation (2.1). This way a good choice of $u^*(0)$ will help to obtain a fast convergence to the optimal solution of the problem (GRÜNE; PANNEK, 2011), (ROSSITER, 2003). In other words, the prediction window shifts foward at each iteration of the MPC algorithm, giving robustness to the control (ABBAS, 2011).

2.2.4 Constraints

One of the major selling aspects of MPC for researches is the capability of dealing with constraints on an intuitive manner. A simple form to describe a linear constraint is

$$U_{min} \leq u(t) \leq U_{max} \tag{2.3a}$$

$$X_{min} \leq x(t) \leq X_{max} \tag{2.3b}$$

where (2.3a) and (2.3b) are upper and lower limits on control inputs and states (ABBAS, 2011). The controller will maximize its efficiency as longs as it operates close to the constraints boundaries.

A disadvantage of using constrained optimization is that sometimes a solution to this type of problem can be infeasible. This way, it is important to take steps when using MPC to avoid this situations, or to have another controller to substitute the control signal provided to the system. According to Maciejowski (2002), some approaches can be considered when designing a constrained MPC. One is to reduce the number of hard constraints. A hard constraint is a constraint that has to be satisfied. It is most used in cases of physical limitations of the system, such as accelerators, valves etc. This avoid a mismatch between the desired output predicted by the system model and the actual output measured. Another possibility is to replace the hard constraints for soft constraints. A soft constraint is a condition that should be satisfied, if possible. Adding a penalty value to the cost function, a soft constraint can be violated in situations where the system will not be in danger (ROSSITER, 2003). Another possible solution is to use alternative solvers for the optimizer.

2.2.5 Optimizer

The system model used in this project is nonlinear. This way, the optimizer has to deal with some issues that are not present on LMPC. In the linear case, the convex quadratic algorithms are in their major part solved at each sampling time. On the contrary, for the NMPC case, either the iteration process runs until a convergence criteria is met, which could add considerable feedback time delay, or the iteration stops at a determined computational time limit, giving only an approximate solution (DIEHL; FERREAU; HAVERBEKE, 2009).

The development of more powerful processors allowed the implementation of real-time optimization algorithms for NPMC, making it possible to be used in real systems. Nowadays, there are many techniques that make use of methods to reduce the computational cost of NMPC algorithms in order to make them faster. The method used in this project is the C/GMRES, that will be detailed on Chapter 4.

2.2.6 Model predictive control in autonomous vehicles

The implementation of model predictive control in autonomous vehicles has rapidly grown over the years with the advance of the computational power. Researchers have been using MPC with constraints on control inputs and state values to guarantee safe and fuel economic trajectories (ZHANG; SPRINKLE; SANFELICE, 2015).

A computational aware autonomous vehicle is controlled by an MPC in (ZHANG; SPRINKLE; SANFELICE, 2015). The authors define the vehicle as computational aware because of the hybrid characteristics of this MPC. The vehicle is controlled with two different models, one being more accurate than the other, which would increase the calculation time for a solution. Whenever the MPC is searching for an optimal solution, it will switch between the two models according with its necessities; if it needs a fast response, the less accurate model will be used and consequentially the error will increase, if it is necessary to reduce the tracking error, the more accurate model would take place and correct the vehicle trajectory.

Abbas, Milman & Eklund (2017) use in their project an NMPC for trajectory tracking with obstacle avoidance of an autonomous ground vehicle at realistic speeds, based on a car model from CarSim. It was noted that the performance of the obstacle avoidance could be increased with a longer prediction horizon, but also elevating the computational burden. The trajectory was planned offline and updated in real time using the NMPC, whenever an obstacle was detected. A low level control scheme, such as PID or LQR was used to control the vehicle actuators. In (DU; HTET; TAN, 2016), an NMPC was applied to an autonomous vehicle for speed and steering control. The main difference in their work is the implementation of a Genetic Algorithm (GA) as the optimization solver. The GA has the advantage of not being limited by convexity and polynomial nonlinearity, which appears in typical control problems. Also, the constraints can be incorporated in the search space during the optimization for the input variables. Both the velocity and steering were controlled simultaneously.

Du, Htet & Tan (2016) proposed a novel heading predictive control model for scenarios where the vehicle is at high speed or needs severe turning. The MPC predicts the best control input for the problem based on a mathematical system model of the vehicle. In order to improve the performance of the algorithm, the non linearity of the tire model was considered in this work, which could improve the vehicle dynamics representation.

To reduce the computational time of the MPC algorithms, Carvalho et al. (2013) developed an MPC for autonomous vehicles using an iterative linearization approach. In this approach, it is obtained an analytic linearization of the nonlinear vehicle dynamics and collision avoidance constraints. Thus, the online computational time compared with other optimization methods, such as GA, could be reduced.

Another application of MPC in autonomous vehicles is present on path planning with clothoids. Lima et al. (2015) use clothoids to allow a smooth driving, varying the steering angle as a linear function, increasing the driving comfort. By calculating the control inputs using the clothoids parameters, a large prediction distance is used without a high computational burden.

2.3 Ecological driving

The increasing of fuel consumption became an issue not only for the drivers, but also for the environmental, since the fuel price and pollutant gases in the atmosphere are arising. The concepts of ecological driving was created to reduce the impact of these problems (BARKENBUS, 2010). The ecological driving, or eco-driving, is a group of strategies that a driver can adopt in order to reduce the fuel consumption of a vehicle, consequentially increasing the driver safety and reduce the number of accidents (BARTH; BORIBOONSOMSIN, 2009). Vaezipour, Rakotonirainy & Haworth (2015) summarized some of the main factors that impact on fuel consumption and safety in Table 1.

Table 1: Fuel consumption and safety driving parameters.

Driving parameters	**Fuel consumption**	**Safety**
Follow speed limit	May increase fuel consumption in low speeds	Decrease risk of accidents
Smooth acceleration	Decrease fuel consumption	Decrease aggressive driving
Smooth deceleration	Decrease fuel consumption	May increase risk of accidents due to short headway
Sharp braking	Increase fuel consumption	May increase risk of accidents due to read-end collision
Aggressive driving	Increase fuel consumption due to hard acceleration and braking inputs	Increase risk of accidents

Source: Vaezipour, Rakotonirainy & Haworth (2015)

The main strategies that the driver can implement for eco-driving are (BARTH; BORIBOONSOMSIN, 2009):

- Avoid driving at high speed;
- Do not accelerate or brake too sharply;
- Shift the gears around 2000 rpm;
- Maintain a constant speed when possible;

- Perform a periodical maintenance on the vehicle;
- Check the tire pressure constantly;

The emergence of new vehicle technologies, engines and energy sources created different ways to improve fuel economy. Also, with the increasing of computational potential, new techniques for control and for the planning in autonomous vehicles are arising. Figure 4 shows an illustration of these new technologies (ZHOU; JIN; WANG, 2016).

Figure 4: New technologies for fuel economy in vehicles.

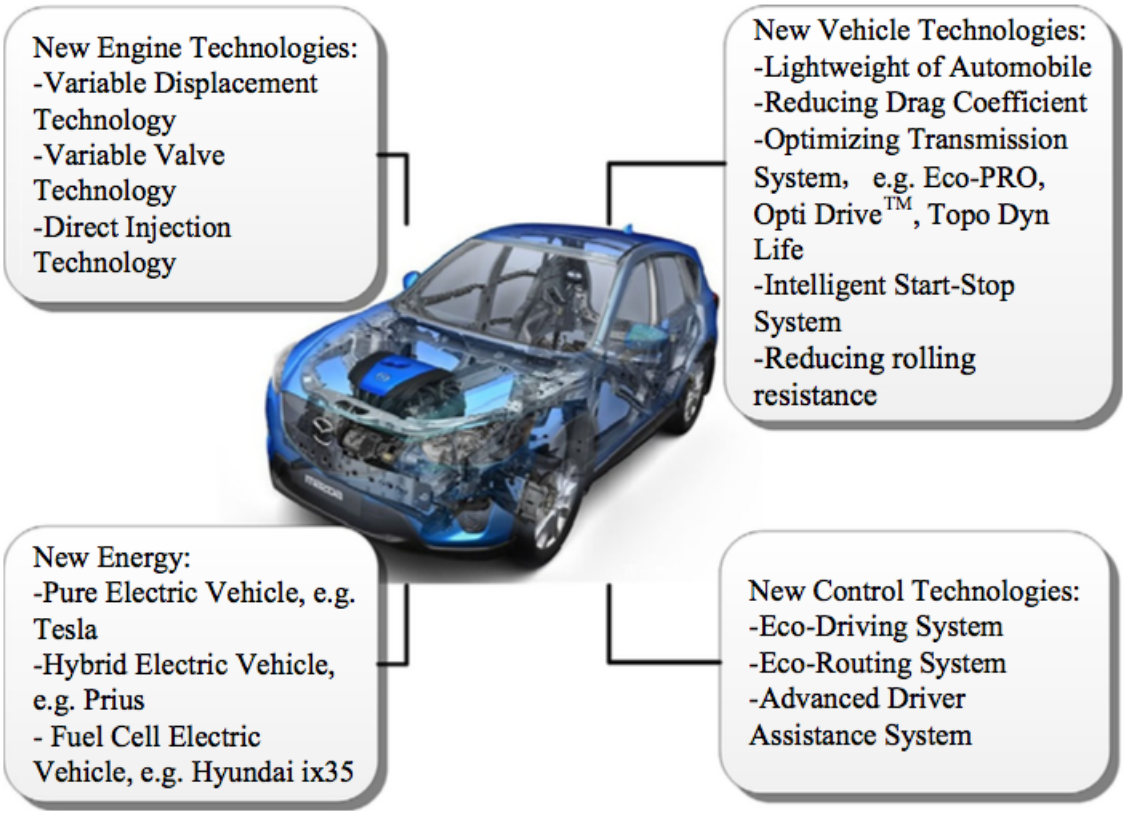

Source: Zhou, Jin & Wang (2016)

The structure diagram in Figure 5 shows the main factors associated with fuel consumption in a vehicle. In travel related factors, the length of a path and the amount of travels within a period of time is considered as the main parameter for reducing the fuel consumption. Yao & Song (2013) uses the Dijkstra route planning approach to find the better solution, by calculating the cost of each route using a mesoscopic vehicle emission and fuel consumption models for light, mid and heavy-duty vehicles. In (KRASCHL-HIRSCHMANN; FELLENDORF, 2012), an energy estimation method indicates the best route for an electrical vehicle (EV), considering the acceleration, driving phase and travel conditions associated in each route.

Figure 5: Diagram of factors that can affect the fuel consumption in a vehicle.

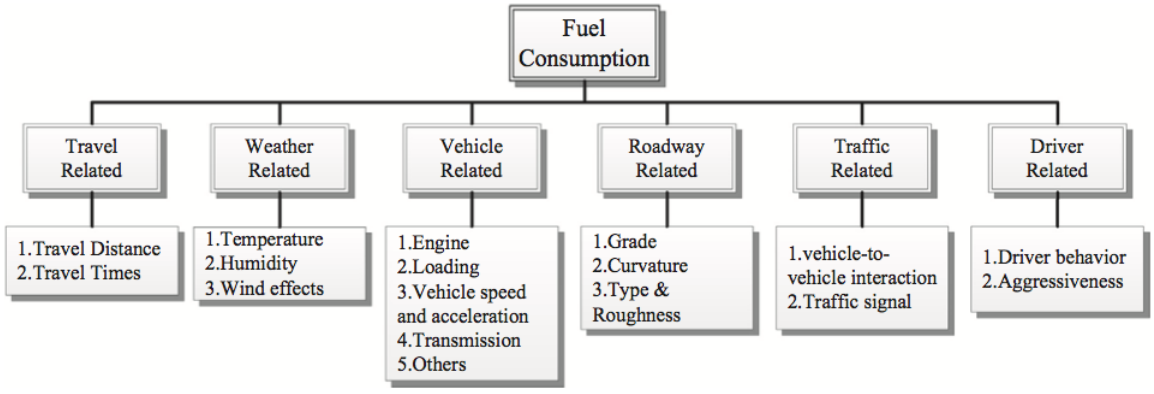

Source: Zhou, Jin & Wang (2016)

The temperature, humidity and the intensity of wind can also impact on fuel consumption. The U.S. Environmental Protection Agency (2015) affirms that an economy of up to 1 % can be achieved by improving the water pump and the air conditioner attachments of the vehicle.

The major part of the fuel economy studies are focused on vehicle-related factors. Ben-Chaim, Shmerling & Kuperman (2013) uses the engine efficiency to estimate the fuel consumption from the vehicle current speed and acceleration. Zhou et al. (2013) collected data from 600 private vehicles and by using pattern recognition features, it could identify the patterns that were affecting the gasoline usage.

In roadway related factors, it is considered the physical characteristics of a road, such as surface roughness and slope. The slope of a route can almost double the fuel consumption of a vehicle, according to Carrese, Gemma & Spada (2013). Works from Vajedi & Azad (2016), Junell & Tumer (2013) and Alrifaee, Liu & Abel (2015) use MPC to optimize the future control inputs of the vehicle in order to reduce sharp acceleration and braking variations. A digital road map of the route is necessary to implement this method, since the controller will use upcoming trip data to adjust the vehicle velocity.

Under traffic-related factors, there are impacts of traffic flow and signalling. The studies developed by Kamal et al. (2013) and Ozatay et al. (2013), for example, use information from the traffic lights state and traffic environment on the trajectory route. This way, the vehicle can adjust its speed or acceleration in order to reduce the fuel consumption, depending on how fast or slow the vehicle can drive.

The driver-related factors are directly referred to driver behavior and aggressiveness, regarding the speed and acceleration profiles. The studies in this area focus on giving the

right training to the population in order to reduce the fuel consumption on their vehicles. Some obtained results in this case are a reduction of 4.6 % in Australia (JEFFREYS; GRAVES; ROTH, 2016), 20 % in France, and 16.9 % in the United Kingdom.

The aggressive driving behavior is the factor that mostly increase the fuel consumption and the accidents rates during a trip. Therefore, the current masters thesis will focus on the implementation of eco-driving strategies with nonlinear model-based predictive control, focusing on reducing fuel consumption and increasing comfort and safety levels.

The main contribution of the present master thesis will be reduce the fuel consumption in autonomous ground vehicles, by considering road-related factors with an NMPC approach. The main difference from the above cited works is that both lateral and longitudinal forces will be considered in the system model, to ensure a safe and economic trip. The specific speed limits of a road segment is also taken into consideration, when the vehicle enters in a different speed limit zone.

3 VEHICLE MODELS

This chapter describes the vehicle models used in this work to address the fuel consumption problem. The vehicle used as a reference for the models presented in this chapter is a Fiat Palio Adventure 1.8 2012, with dualogic gearbox, called Carina 2, which is showed in Figure 6. This vehicle was used to collect data using a computer with Robot Operating System (ROS), connected to the CAN (Controller Area Network) bus of the vehicle. Such data is necessary in order to calibrate and evaluate the model presented in this chapter.

Figure 6: Autonomous vehicle Carina 2.

Source: Mobile Robotics Lab - LRM, 2012.

3.1 Vehicle dynamic model

The longitudinal motion of a vehicle at time t can be described by the state equation of the system (3.1). The state vector and the control input are $x(t)$ and $u(t)$, respectively.

$$\dot{x}(t) = f(x(t), u(t)) \tag{3.1}$$

The state vector $x(t)$ of the vehicle is represented by (3.2), where $s(t)$ is the travelled distance in meters, and $v(t)$ the velocity, in meters per second (m/s). The control input $u(t)$ represents the tractive input of the vehicle in Newton per kilogram, where a positive value corresponds to the throttle pedal being used and negative for the brake pedal.

$$x(t) = [s(t), v(t)]^T \tag{3.2}$$

The Newton's second law is used to calculate the acceleration along the longitudinal direction of the vehicle, assuming a point mass at the center of gravity. Thus, the sum of all forces acting on the vehicle can be given by Equation (3.3). According to Sajadi-Alamdari, Voos & Darouach (2016), these forces are the traction force $F(t)$, the rolling resistance force F_{roll}, the gravitational force F_{grav} and the aerodynamic drag force F_{drag}, given by Equation (3.4). The in add parameters are the vehicle mass M, the gravitational acceleration g, the road slope angle $\theta(s)$ at position s, the aerodynamic drag coefficient C_D, the air density ρ, and the frontal area of the vehicle A_f. Equation (3.5) represents the rolling resistance coefficient for passenger vehicles, assuming the road has a concrete surface. An illustration of acting forces on the vehicle can be seen in Figure 7.

Figure 7: Longitudinal dynamic model of the vehicle.

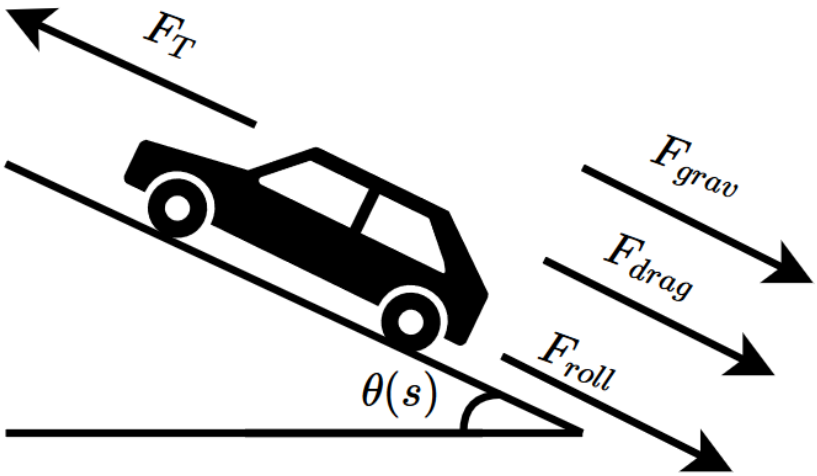

Source: Author.

$$M\dot{v}(t) = F_T(t) - F_{roll}(t) - F_{drag}(t) - F_{grav}(t) \tag{3.3}$$

$$F_T(t) = Mu(t), \tag{3.4a}$$
$$F_{roll}(t) = C_{rr}(v)Mg\cos(\theta(s)), \tag{3.4b}$$
$$F_{grav}(t) = Mg\sin(\theta(s)), \tag{3.4c}$$
$$F_{drag}(t) = \frac{1}{2}C_D\rho A_f v^2 \tag{3.4d}$$

$$Crr(v) = 0.01(1 + v/576) \tag{3.5}$$

Therefore, the state equation of the system can be rewritten as

$$\begin{bmatrix} \dot{s} \\ \dot{v} \end{bmatrix} = \begin{bmatrix} v \\ u - \frac{1}{2M} C_D \rho A_f v^2 - g\sin(\theta(s)) - C_{rr}(v) g\cos(\theta(s)) \end{bmatrix}, \tag{3.6}$$

where the vehicle acceleration is represented by $\dot{v} = a$ later on this work.

This work assumes that a digital road map is available for the driver, in order to obtain the slope profile and road curvature information along the path to ensure a safe and comfortable trip. Therefore, the road slope angle, in radians, can be calculated as

$$\theta(s) = \tan^{-1}\left(\frac{R_{alt}(s + \Delta s) - R_{alt}(s - \Delta s)}{2\Delta s}\right), \tag{3.7}$$

where R_{alt} is the road altitude information obtained from the digital road map for a given location. A fixed distance, Δs is used to approximate the slope angle by the difference between the altitude in two different positions.

Although this work only approach the longitudinal control of the autonomous vehicle, the lateral acceleration existent during steering has a significant impact on the driver's comfort. Therefore, a relation between the road curvature and the vehicle velocity must be established in order to maintain a safe and comfortable trip. The lateral acceleration of the vehicle during steering is related to the road absolute curvature profile, calculated by

$$f_{curv}(s) = \left|\frac{1}{R_{curv}(s)}\right|. \tag{3.8}$$

where R_{curv} is the radius of the curve. Therefore, the lateral acceleration acting on the vehicle can be expressed by

$$a_{lat} = v^2 f_{curv}(s). \tag{3.9}$$

The engine speed of the vehicle is given by

$$\omega_e(t) = \min\left(\max\left(\frac{1000 v(t) \xi}{120\pi r(1 - i)}, \omega_{idle}\right), \omega_{red}\right) \tag{3.10}$$

where ξ, r, ω_{idle}, ω_{red} and i are the current gear ratio, wheel radius, engine speed at idle, redline engine speed and tire slipage percentage, respectively. These parameters can be found in the vehicle's manual.

The engine speed of the vehicle is proportional to its velocity, and it is an important parameter when estimating the instant fuel consumption and gear shifting. Therefore, a comparison between simulated and measured data was performed to validate Equation (3.10), by using the same velocity profile. The results obtained are shown in Figure 8, where it is possible to achieve a correlation coefficient of $R = 0.9625$.

Figure 8: Simulated and measured engine speed comparison.

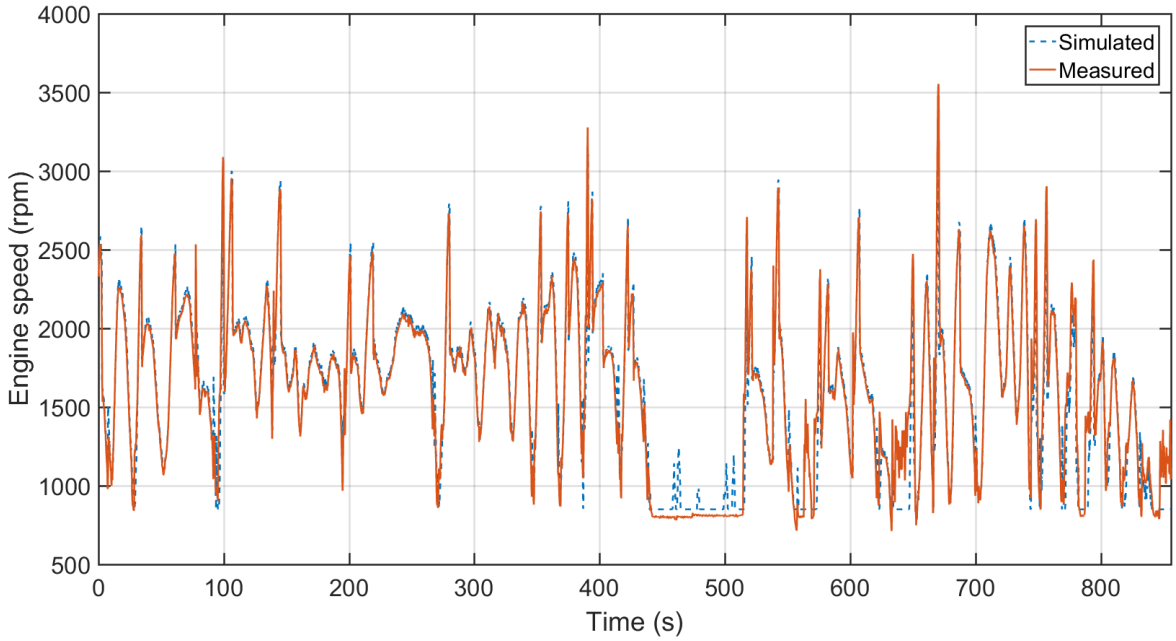

Source: Author.

3.2 Gear shifting model

The vehicle traction power and, consequently, the fuel consumption are affected by which current gear the engine is operating. In order to properly evaluate the need to shift gears during a trip, a combination of field data and the vehicle specifications were used to design a gear shifting model.

The gear control policy is based in various factors, such as throttle position, engine speed and vehicle velocity (RAKHA et al., 2012). To simplify the calculations, only engine speed and vehicle velocity were considered in this model. A decision tree algorithm with 30 branches in combination with vehicle field data is used to find the best gear shifting points. The training and testing of the decision tree algorithm was performed using MATLAB classification learner application. The results obtained are presented in Figure 9, where a correlation coefficient of $R = 0.962$ was achieved.

A decision tree algorithm was chosen for this model because the vehicle did not achieved the fifth gear during the tests and could not be included in the training process.

Figure 9: Predicted gears using a decision tree with 30 branches.

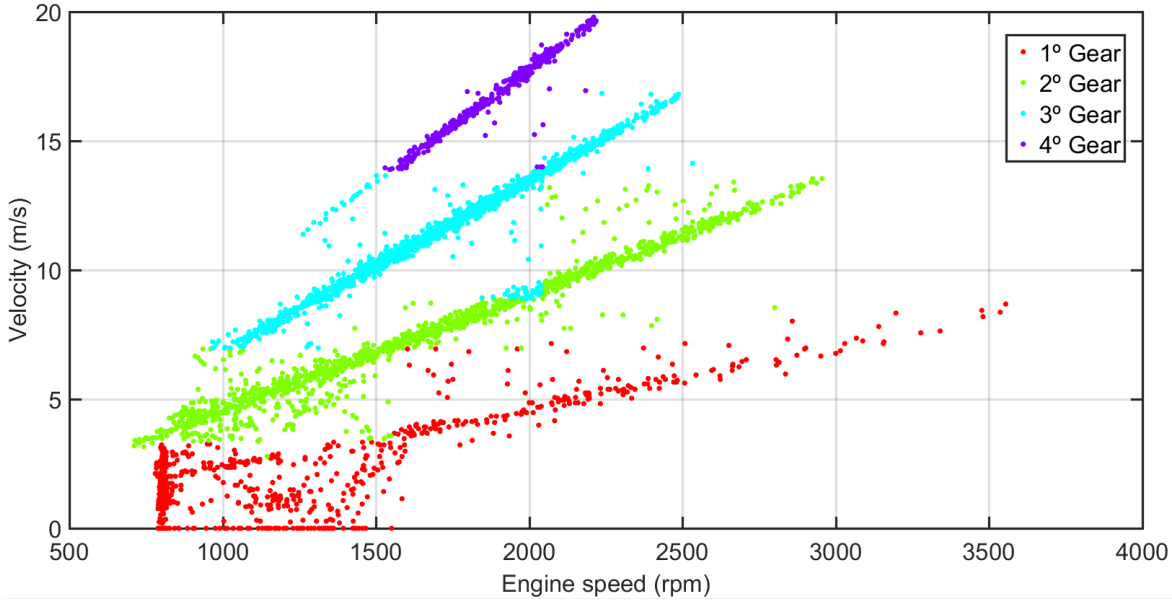

Source: Author.

In order to avoid this issue, the vehicle specifications were used in combination with the field data to increase the complexity of the decision tree in 4 additional branches. The resulting decision tree is shown in Figure 10.

3.3 Fuel consumption model

There are many vehicle fuel consumption models in the literature, but most of them suffer from two major drawbacks in their usage. The first is that they produce a bang-bang control, which would indicate that the optimal fuel economy is achieved at full throttle to reduce the acceleration time. The second problem is the need of field and laboratory data in order to calibrate the model parameters, since these tests are very time consuming, expensive and require a good vehicle instrumentation. To avoid these issues, the fuel consumption model used in this work is the VT-CPFM-2, developed by Rakha et al. (2011). The main advantage is that it only requires publicly available fuel consumption and vehicle driveline data.

The vehicle power, given by Equation (3.11), is obtained by the product of the required force necessary to overcome the resistances forces and the vehicle velocity. The term $(1.04 + 0.0025\xi(t)^2)$ represents the moment of inertia of the vehicle for a given gear ratio ζ (WONG, 2001). The driveline efficiency of the vehicle is represented by η_d.

$$P(t) = \left(\frac{F_{roll}(t) + F_{drag}(t) + F_{grav}(t) + Ma(t)(1.04 + 0.0025\xi(t)^2)}{3600\eta_d} \cdot v(t) \right) \tag{3.11}$$

Figure 10: Decision tree for gear shifting based on engine speed ω_e (RPM) and vehicle velocity v (m/s)

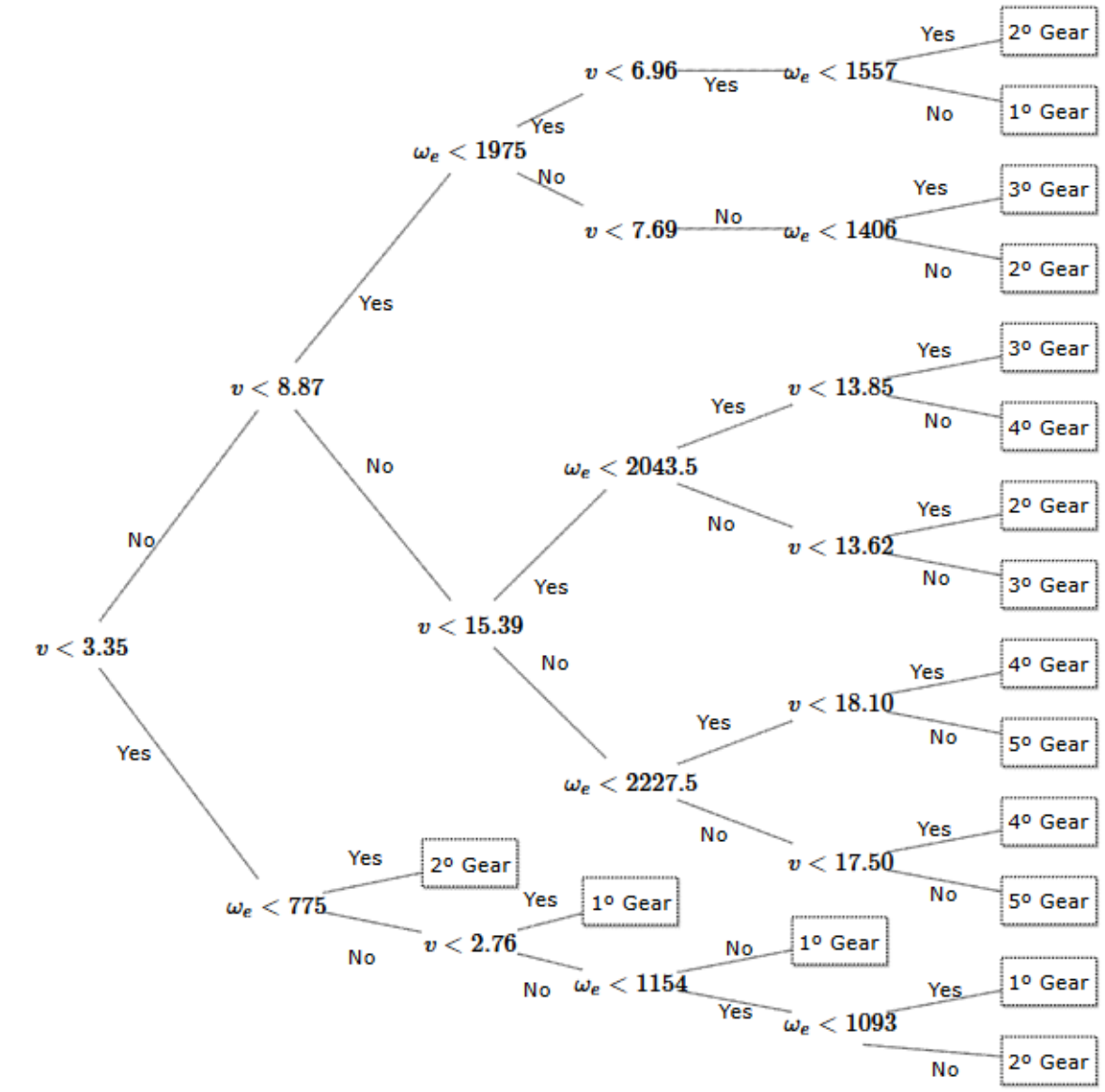

Source: Author.

The instant fuel consumption of a vehicle, in liters per second, is given by

$$FC(t) = \begin{cases} \beta_0 \omega_e(t) + \beta_1 P(t) + \beta_2 P(t)^2, & \text{if } P(t) \geq 0 \\ \beta_0 \omega_{idle}, & \text{if } P(t) < 0 \end{cases} \tag{3.12}$$

where β_0, β_1 and β_2 are vehicle-specific constants, calibrated for each vehicle.

The US Environmental Protection Agency (EPA) cycles for fuel consumption estimation in city and highway are used to calibrate the fuel consumption model equations. In Equation (3.12), the first constant β_0 represents the idling fuel consumption rate, calculated by Equation (3.13), where P_{mfo} is the idling fuel pressure (400,000 Pa), d the

engine displacement in liters, Q the fuel lower heating value (43,000,000 J/kg for gasoline), N_{cil} the number of engine cylinders, F_{city} and F_{hwy} are the fuel consumption estimation by the vehicle manual in liters for city and highway. The engine cycles used during fuel economy ratings for city and highway, ω_{city} and ω_{hwy}, are given by Equation (3.16), where P_{city} and P_{hwy} are the sum of power exerted each second over the entire cycle, described in Equation (3.17). The duration of the EPA cycles for city and highway, 1875 and 766 seconds, are represented by T_{city} and T_{hwy}. Constants in Equation (3.18) and Equation (3.19), 3.7854 and 1.6093, are the conversion factor from gallon to liters and miles to kilometers. The distance traveled in the city and highway cycles are 17.663 and 16.4107 km, respectively.

$$\beta_0 = \max\left(\frac{P_{mfo}d}{22164 \cdot QN_{cil}}, \frac{(F_{city} - F_{hwy}) - \varepsilon(P_{city}^2 - P_{hwy}^2\frac{P_{city}}{P_{hwy}})}{\omega_{city} - \omega_{hwy}\frac{P_{city}}{P_{hwy}}}\right) \tag{3.13}$$

Equation (3.15) has to be greater than 1×10^{-06}, since experimentation with the model showed that this value ensures that the fuel economy cruising velocity at optimal condition is around 60-80 km/h for light-duty vehicles (RAKHA et al., 2011). At last, Equation (3.14) computes the second constant β_1. A MATLAB tool is used to calculate the constants used in the fuel consumption model.

$$\beta_1 = \frac{\left(\frac{F_{city} - \omega_{city}\beta_0 - P_{city}^2\beta_2}{P_{city}}\right) + \left(\frac{F_{hwy} - \omega_{hwy}\beta_0 - P_{hwy}^2\beta_2}{P_{hwy}}\right)}{2} \tag{3.14}$$

$$\beta_2 = \frac{(F_{city} - F_{hwy}) - (\omega_{city}^2 - \omega_{hwy}^2\frac{P_{city}}{P_{hwy}})\beta_0}{P_{city} - P_{hwy}\frac{P_{city}}{P_{hwy}}} \geq 1 \times 10^{-06} \tag{3.15}$$

$$\omega_{city} = \sum_{t=0}^{T_{city}} \omega(t) \quad \text{and} \quad \omega_{hwy} = \sum_{t=0}^{T_{hwy}} \omega(t) \tag{3.16}$$

$$P_{city} = \sum_{t=0}^{T_{city}} P(t) \quad \text{and} \quad P_{hwy} = \sum_{t=0}^{T_{hwy}} P(t) \tag{3.17}$$

$$F_{city} = \frac{3.7854 \times 17.663}{1.6093 \times FE_{city}} = \frac{41.5546}{FE_{city}} \tag{3.18}$$

$$F_{hwy} = \frac{3.7854 \times 16.4107}{1.6093 \times FE_{hwy}} = \frac{38.6013}{FE_{hwy}} \tag{3.19}$$

The second term of Equation (3.12) refers to the instant fuel consumption of the vehicle when it is decelerating in neutral gear. This scenario is called coasting (ECKHOFF; HALMOS; GERMAN, 2013). In this case, the vehicle gearbox is disconnected from the powertrain and its velocity reduces due the aerodynamic force. Fuel is still consumed to maintain the engine rotating at the idle rpm (ω_{idle}). Another possible scenario, called engine braking, is when the driver does not press either the brake or throttle pedal and also does not put in the neutral gear, keeping the gearbox and the powertrain still connected. This way, the vehicle kinetic energy that will drive the engine speed and the internal friction works as a brake force. The electronic fuel injection system cuts the fuel consumption until it reaches a point where the vehicle stalls due lower velocity levels (SAERENS, 2012). In this work, since the automatic gearbox controls the gear selection and will not go to neutral when decelerating, the engine brake scenario is considered. Therefore, $FC(t) = 0$ when $P(t) < 0$.

In terms of fuel economy, coasting is only recommended at higher velocities ($v > 90km/h$). According to Eckhoff, Halmos & German (2013) and Saerens (2012), in engine braking the vehicle velocity will drop much faster than when it is coasting, which can cause the driver to accelerate more and increase the fuel consumption.

4 NONLINEAR MODEL PREDICTIVE CONTROL

This chapter details the nonlinear model predictive controller used in this work. Applications in autonomous vehicles requires a fast algorithm to guarantee real-time implementation, so the selection of the optimizer used during the calculation is very important. It will cover the constraints, the cost function and the execution of the C/GMREs algorithm. An illustration of the concept of the control system is represented in Figure 11.

Figure 11: Illustrated concept of the control system.

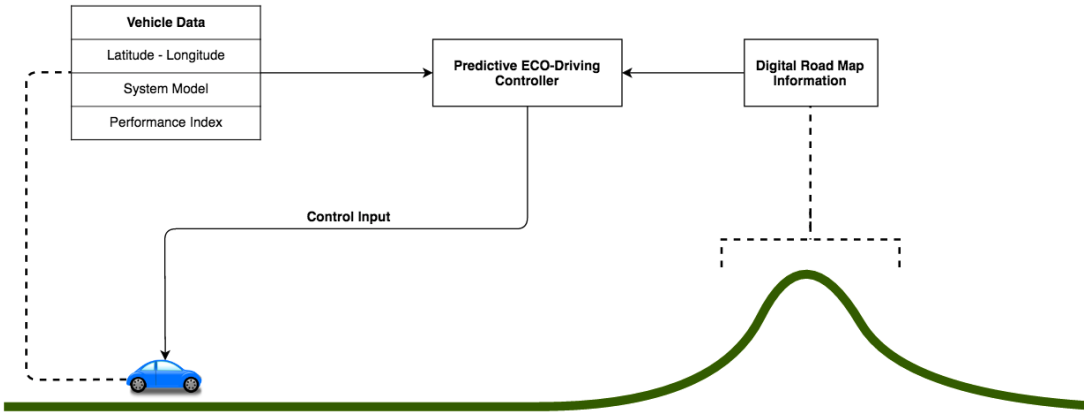

Source: Author.

4.1 Constraints

The traction force of the vehicle $F_T(t)$, according to Rakha et al. (2012), should be less than the maximum frictional force that can be sustained between the vehicle's wheels on the propulsive axle and the road surface. This constraint is represented in Equation (4.1), where M_{ta} is the mass of the propulsive axle in kg and γ the road adhesion.

$$F_T(t) < \gamma M_{ta} g \tag{4.1}$$

Therefore, there is an input constraint as

$$-\frac{\gamma M_{ta} g}{M} \leq u \leq \frac{\gamma M_{ta} g}{M} \tag{4.2}$$

which ensures the vehicle does not slip during acceleration or braking.

The inequality constraint from Equation (4.2) can be converted to an equality constraint by introducing a slack input u_{slk} as follows

$$C(x(t), u(t), p(t)) = \frac{(u^2 + u_{slk}^2 - u_{max}^2)}{2} = 0. \tag{4.3}$$

The slack input is square to constrain the sign of $u^2 - u_{max}^2$ to be negative. To avoid a singularity when finding a solution for $u_{slk} = 0$, a small penalty is added to the cost function, as it will be shown in section 4.2.

4.2 Cost function

The stage cost L used in this work is given by

$$L(x, u, p) = L_1 + L_2 + L_3 + L_4 + L_5 + L_6 - L_{slk}, \tag{4.4}$$

where each term represents one objective.

In order to minimize the acceleration and braking levels needed to counterbalance the gravitation force in up-down slope sections of the road, Equation (4.5) is used. Thus, the vehicle will increase its velocity before entering an elevated slope section and control the deceleration levels when at a downhill.

$$L_1 = w_1 \left[\frac{1}{2} \Big(a + g \cdot sin(\theta(s)) \Big)^2 \right] \tag{4.5}$$

The cost of the Equation (4.6) will increase when the vehicle deviates from the reference velocity v_{Ref}. This helps avoiding the vehicle to stop during the trip.

$$L_2 = w_2 \left[\frac{1}{2} \left(v - v_{Ref} \right)^2 \right] \tag{4.6}$$

The following three cost function terms are in exponential form because their cost will not rise when the difference between the measured and reference values are negative. To ensure a safe and comfortable trip, the costs given by Equation (4.7) and (4.8) penalize elevated levels of longitudinal and lateral accelerations. Equation (4.9) ensures the vehicle velocity is lower than the maximum allowed speed in a road or highway.

$$L_3 = e^{w_3(a - a_{var})} \tag{4.7}$$

$$L_4 = e^{w_4(v^2 f_curv(s) - a_{latMax})} v^2 \tag{4.8}$$

$$L_5 = e^{w_5(v - v_{lim})} v \tag{4.9}$$

The sixth term given by Equation (4.10) will help to chose the velocity that will minimize the fuel consumption rate at a steady condition. The last term, L_{slk}, is inserted to avoid singularities when calculating the optimal control input due the partial differentiation of the Hamiltonian. The weighting constants $w_i, i = 1..6$ are used to balance the magnitude cost of each term of the cost function correctly.

$$L_6 = w_6 \left[\frac{\beta_0 \omega_e(t) + \beta_1 P(t) + \beta_1 P(t)^2}{2v} \right] \tag{4.10}$$

$$L_{slk} = w_{slk} u_{slk} \tag{4.11}$$

4.3 C/GMRES

The C/GMRES algorithm is a combination of the continuation method with a linear equation solver called generalized minimum residual (GMRES) method, instead of using Riccati differential equations. Based on the state equation, stage cost and system constraints, the Hamiltonian H can be defined as

$$H(x, \lambda, u, \mu, p) = L(x, u, p) + \lambda^T f(x, u, p) + \mu^T C(x, u, p). \tag{4.12}$$

where λ is the costate and μ the Lagrange multiplies associated with the equality constraint from Equation (4.3).

The road slope angle depends of information on the digital map, and it is in function of only the traveled distance $x_1 = s$. For this optimal control problem, to derive the control input it is required to calculate the following

$$\begin{aligned} H_s &= \frac{\partial}{\partial s} H(x, \lambda, u, \mu) \\ &= \frac{\partial}{\partial s} (L(x, u) + \lambda^T f(x, u) + \mu^T C(x, u) \\ &= \lambda_2 g \cos\theta(s) \frac{d}{ds} \theta(s). \end{aligned}$$

Therefore, using the Equation (3.7) to obtain the road slope angle, $d/ds\theta_s$ can be computed as

$$\frac{d}{ds}\theta(s) = \frac{\theta(s + \Delta s) - \theta(s - \Delta s)}{2\Delta s}. \tag{4.13}$$

The control input is determined in order to minimize the performance index with a prediction horizon as following

$$J = \phi(x(t + T), p(t + T)) + \int_t^{t+T} L(x(\tau), u(\tau), p(\tau)) d\tau. \tag{4.14}$$

Using the Hamiltonian, it is possible to replace the cost function term in the expanded performance index as

$$J = \phi(x(t+T), p(t+T)) + \int_t^{t+T} (H(x, \lambda, u, \mu, p) - \lambda^T \dot{x}) d\tau. \tag{4.15}$$

This way, the necessary conditions for the optimal solution are given by the following Euler-Lagrande equations

$$\dot{x}(t) = f(x(t), u(t), p(t)), \quad x(t) = x_0(t) \tag{4.16}$$
$$\dot{\lambda}(t) = -H_x^T(x(t), \lambda(t), u(t), \mu(t),), \tag{4.17}$$
$$\lambda(t+T) = \phi_x(x(t+T), p(t+T)), \tag{4.18}$$
$$H_u(x(t), \lambda(t), u(t), \mu(t), p(t)) = 0 \tag{4.19}$$
$$C(x(t), u(t), p(t)) = 0. \tag{4.20}$$

The horizon is divided into N as $\Delta\tau = \frac{T}{N}$. Thus, the optimal control problem can be discretized with the forward difference on the τ axis as

$$x_{i+1}^*(t) = x_i^*(t) + f(x_i^*(t), u_i^*(t))\Delta\tau, \quad x_0^*(t) = x(t), \tag{4.21}$$
$$\lambda_i^*(t) = \lambda_{i+1}^*(t) + H_x^T(x_i^*(t), \lambda_{i+1}^*(t), u_i^*(t), \mu_i^*(t), p_i^*(t))\Delta\tau, \tag{4.22}$$
$$\lambda_N^*(t) = \phi_x^T(x_N^*(t), p_N^*(t)), \tag{4.23}$$
$$H_u^T(x_i^*(t), \lambda_{i+1}^*(t), u_i^*(t), \mu_i^*(t)) = 0 \tag{4.24}$$
$$C(x_i^*(t), u_i^*(t), \mu_i^*(t), p_i^*(t)) = 0, \tag{4.25}$$

A two-point boundary value problem (TPBVP) is defined when the sequences of the optimal control and the multiplier satisfies the conditions from Equation (4.21) to Equation (4.25). This way, the TPBVP for discrete problems is identical to a finite difference approximation of the TPBVP continuous-time problem.

A vector of the input and multipliers can be defined as

$$U(t) = [u_0^{*T}(t), \mu_0^{*T}(t), ..., u_{N-1}^{*T}(t), \mu_{N-1}^{*T}(t)]. \tag{4.26}$$

Since $x_i^*(t)$, $\lambda_{i+1}^*(t)$ can be calculated recursively and determined by $x(t)$ and $U(t)$ through Equation (4.21) to Equation (4.23), Equation (4.24) and Equation (4.25) can be regarded as one equation and defined as

$$F(U(t), x(t), t) = \begin{bmatrix} H_u(x_0(t), \lambda_1(t), u_0(t), \mu_0(t)) \\ C(x_0(t), u_0(t)) \\ \cdot \\ \cdot \\ H_u(x_{N-1}(t), \lambda_N(t), u_{N-1}(t), \mu_{N-1}(t)) \\ C(x_{N-1}(t), u_{N-1}(t)) \end{bmatrix} = 0 \tag{4.27}$$

Equation (4.27) can be solved at each time t for the measured system state $x(t)$ with respect to $U(t)$ to determine the control input $u(t)$. The solution to this equation using an iterative method such as Newton's method can increase the computational burden considerably. Instead, $U(0)$ is chosen for the following conditions

$$\dot{F}(U(t), x(t), t) = -\zeta F(U(t), x(t), t) \quad (\zeta > 0) \tag{4.28}$$

$$F(U(0), x(0), 0) = 0 \tag{4.29}$$

where ζ is added to stabilize $F = 0$. Therefore, being the Jacobian of F_U nonsingular, a differential equation of $U(t)$ can be obtained as

$$\dot{U} = F_U^{-1}(-F_x - F_t - \zeta F). \tag{4.30}$$

This way, the solution $U(t)$ of $F(U(t), x(t), t) = 0$ can be updated without iterative optimization methods by integrating Equation (4.30) in real time, which is a kind of the continuation method (OHTSUKA, 2004).

To reduce the computational burden of complex operation, such as obtaining the Jacobians F_U, F_x and F_t and F_U^{-1}, two methods are used: forward difference approximation and GMRES for linear equation. The first step is to approximate the product of the Jacobians as

$$F_U(U, x, t)\delta_U + F_x(U, x, t)\delta_x + F_t(U, x, t)\delta_t \simeq D_h F(U, x, t : \delta_U, \delta_x, \delta_t)$$

$$D_h F(U, x, t : \delta_U, \delta_x, \delta_t) := \frac{F(U + h\delta_U, x + h\delta_t, t + h\delta_x) - F(U, x, t)}{h},$$

where h is a positive real number. This way, Equation (4.28) can be approximated by

$$D_h F(U, x, t : \dot{U}, \dot{x}, 1) = -\zeta F(U, x, t)$$

which is identical to

$$D_h F(U, x + h\dot{x}, t + h : \dot{U}, 0, 0) = b(U, x, \dot{x}, t) \tag{4.31}$$

where

$$b(U, x, \dot{x}, t) = -\zeta F(U, x, t) - D_h F(U, x + h\dot{x}, t + h : 0, \dot{x}, 1)$$

The GMRES method can now be applied in Equation (4.31), since it approximates a linear equation with respect to $\dot{U}$. One way to initialize U_0 is choosing the horizon $T(t)$ as

$$T(0) = 0$$

$$T(t) \to T_f (t \to \infty),$$

then $u_i^*(0) = u(0)$, $\mu_i^*(0) = \mu(0)(i = 0, ..., N-1)$ and $x_i^*(0) = x(0)$. This way, the inialization is reduced to finding $u(0)$ and $\mu(0)$ that can satisfy the following inequality

$$\left|\left|\begin{bmatrix} H_u^T(x_0), \phi_x^T(x(0)), u_0, \mu_0) \\ C(x_0(t), u_0(t)) \end{bmatrix}\right|\right| \leq \frac{\delta}{\sqrt{N}},$$

which requires much less computational time than using Equation (4.27).

The C/GMRES method is described in Algorithm 1, where Δt is the sampling period and l is the suffix for short hereafter. The Forward Difference Generalized Minimal Residual (FDGMRES) function is detailed with its mathematical proofs in Ohtsuka (2004).

Algorithm 1: C/GMRES

Set t = 0; $x_0 = x(0)$; $l = 0$;
Find U_0 analytically or numerically that satisfies $||F(U_0, x_0, 0)|| \leq \delta$ for a positive δ;
For $t' \in [t, t + \Delta t]$, set $u(t') = (U(l))$;
At time $t + \Delta t$ measure $x(l + 1) = x(t + \Delta t)$, set $\Delta x_l = x(l + 1) - x(l)$;
Compute $\dot{U}_l = \text{FDGMRES}(U, x, \dot{x}, \hat{\dot{U}}, h, k_{max})$
Function `FDGMRES`$(U, x, \dot{x}, \hat{\dot{U}}, h, k_{max})$**:**
    $\hat{r} = b(U, x, \dot{x}, t) - D_h F(U, x + h\dot{x}, t + h : 0, \dot{x}, 1)$;
    $v_1 = \hat{r}/||\hat{r}||$;
    $\rho = ||\hat{r}||$;
    $\beta = \rho$;
    $k = 0$;
    while $k < k_{max}$ **do**
        $k = k + 1$;
        $v_{k+1} = D_h F(U, x + h\dot{x}, t + h : v_k, 0, 0)$;
        for *j=1:k* **do**
            $h_{jk} = v_{k+1}^T v_j$;
            $v_{k+1} = v_{k+1} - h_{jk} v_j$;
        end
        $h_{k+1,k} = ||v_{k+1}||$;
        For $e_1 = [1\,0...\,0]^T \in \mathbb{R}^{k+1}$ and $H_k = (h_{ij}) \in \mathbb{R}^{(k+1)\times k}$ ($h_{ij} = 0$ for$i > j + 1$, minimize $||\beta e_1 - H_k y^T$ to determine $y^k \in \mathbb{R}^k$;
        $\rho = ||\beta e_1 - H_k y^T$
    end
    $\dot{U} = \hat{\dot{U}} + V_k y^k$, where $V_k = [v_1 ... vk]$;
    return $\dot{U}$;
Set $t = t + \Delta t, l = l + 1$, and repeat from step 3

5 RESULTS

The proposed eco-driving controller was evaluated in simulations using real world digital maps. The vehicle parameters and the NMPC controller settings are shown in Table 2 and Table 3, respectively.

Table 2: Vehicle parameters.

Description	Parameter	Value
VT-CPFM-2 constants	β_0	1.7911×10^{-7}
	β_1	8.284×10^{-5}
	β_2	1×10^{-6}
Mass	M	$1204kg$
Propulsive axle mass	M_{ta}	$782.60kg$
Frontal area	A_V	$2.32m^2$
Drag coefficient	C_D	0.35
Idle engine speed	ω_i	850
Redline engine speed	ω_{red}	5250
Wheel radius	r	$0.381m$
Gear ratios	ξ_1	3.909
	ξ_2	2.238
	ξ_3	1.520
	ξ_4	1.156
	ξ_5	0.909
Final drive ratio	ξ_f	4.607
Driveline efficiency	η_d	0.89

Source: Author.

A prediction horizon of 10 seconds was used in the simulations, divided in 100 steps of size 0.1. The maximum control input allowed by the constraint detailed in chapter 4 is 5.10 N/kg, but since reaching this propulsive force could greatly increase the risk of accidents, the actual control input is limited to $|u| \leq 4.5$. The longitudinal and lateral acceleration constraint levels were chosen based on previous works (KAMAL et al., 2011), (SAJADI-ALAMDARI; VOOS; DAROUACH, 2016). The weighting gains of the cost function were chosen after numerous simulations, to achieve fuel economy during the trip within a comfortable and safe operating levels.

The velocity for the FDS controller is computed by

$$Velocity_{FSD} = \frac{(|Curv(s)| - max(|Curv_{route}|) * (SpeedLimit - 10)}{max(|Curv_{route}|)} + 10, \tag{5.1}$$

where the same system equation for the EDC controller is used during the calculations. The same control input constraint is used due to vehicle limitations and to obtain a realistic comparison.

Table 3: NMPC parameters.

Description	Parameter	Value
Prediction horizon	T	10s
Iteration number in C/GMRES	$kmax$	10
Step size	h	0.1
Range of input	u	[-4.5,4.5]N/kg
Range of longitudinal acceleration	a	[-2.5,2.5]m/s^2
Range of lateral acceleration	a_{lat}	[-3.7,3.7]m/s^2
Road slope angle ratio	Δs	$20m$
Desired constant velocity	v_{Ref}	(Speed limit -10)km/h
	w_1	20
	w_2	0.5
	w_3	1
Cost function weights	w_4	1
	w_5	1
	w_6	3000
	w_{slk}	0.25

Source: Author.

The simulations were performed in MATLAB 2016a, using a laptop with Intel Core i7 - 4810MQ CPU 2.80GHz processor, 12GB RAM and Windows 10 Pro.

5.1 Simulation in a highway scenario

The evaluation of the Eco-driving control algorithm in this section will be compared with a fixed speed cruise controller, which tries to keep the vehicle at the maximum allowed speed of the route for the entire trip (KAMAL et al., 2011). For nomenclature simplicity, in the following Figures the Eco-driving controller and the fixed speed cruise controller will be called EDC and FSD, respectively.

The first scenario considered is a 27km highway route from São Carlos to Araraquara, with map and altitude profile shown in Figure 12. The longitude and latitude data were collected using an API from Google Maps. This route was chosen due an interesting elevation profile; there is a 200m difference between the highest and lowest point, and because of the speed limits variations.

Four different speed limits are considered during the trip: $v_{lim} = 80km/h$ at $s = 0km$, $v_{lim} = 110km/h$ at $s = 3km$, $v_{lim} = 80km/h$ at $s = 20km$ and $v_{lim} = 110km/h$ at $s = 23km$. These speed limits are represented by yellow dashed lines. The presence of others vehicles was not considered during the simulations. Figure 13, 15 and 16 show the results obtained regarding the velocity, slope and curvature profile, longitudinal and lateral acceleration and the fuel consumption for both controllers. A detailed result of the simulation is presented in Table 4. The computational time for the EDC controller is less

than half of the elapsed time in the simulation, which evaluates the proposed algorithm for a real time implementation.

Figure 12: Simulation highway map from São Carlos to Araraquara.

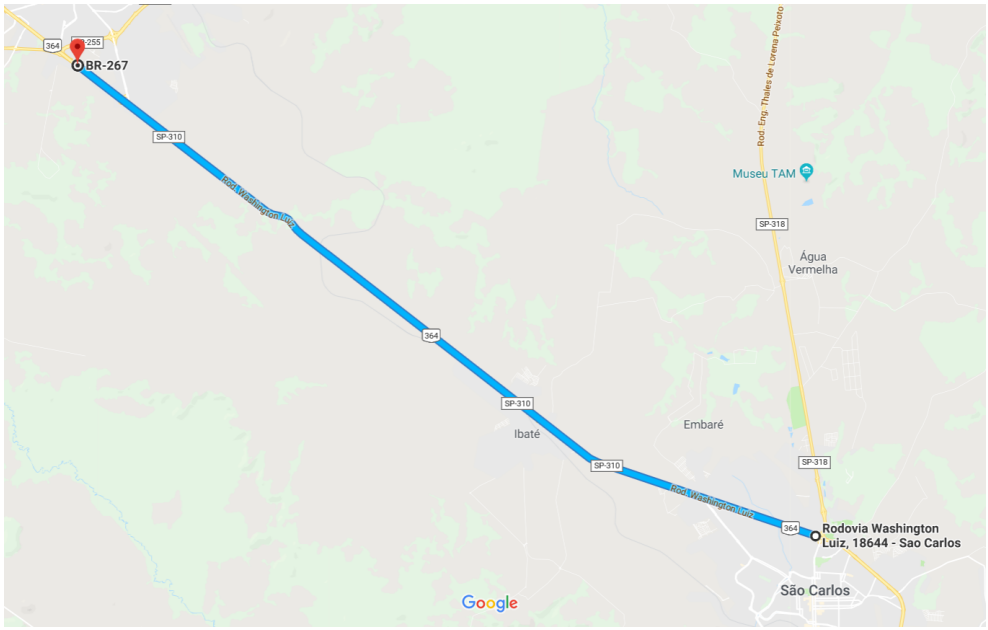

(a) Highway test map.

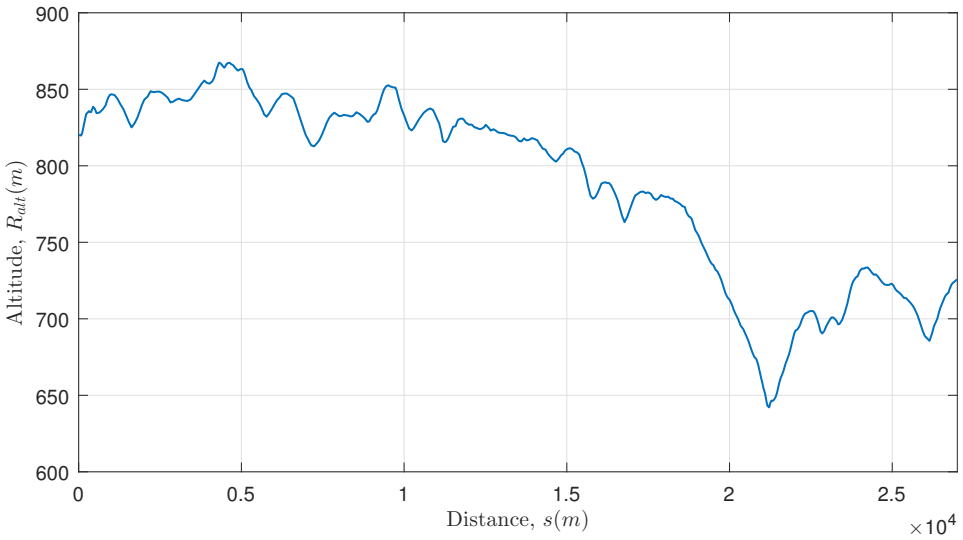

(b) Altitude profile.

Source: Author.

Figure 13: Velocity, slope and curvature profile for the highway scenario.

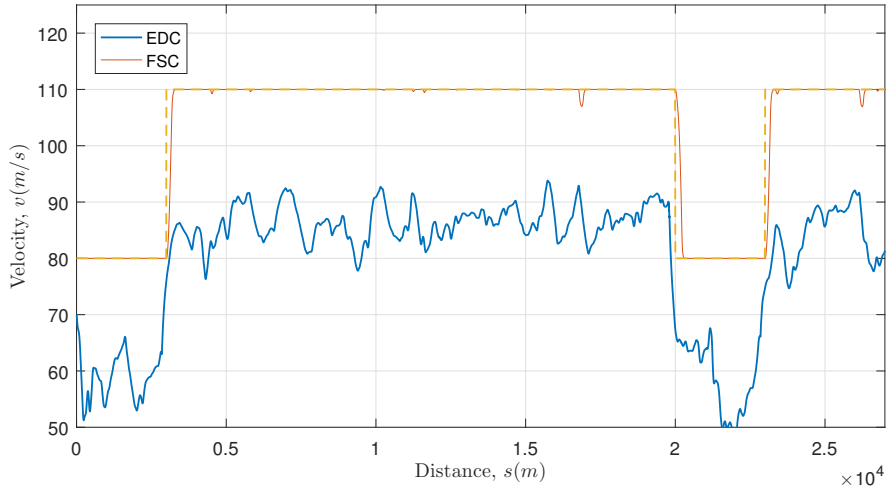

(a) Velocity performance of the Eco-driving algorithm.

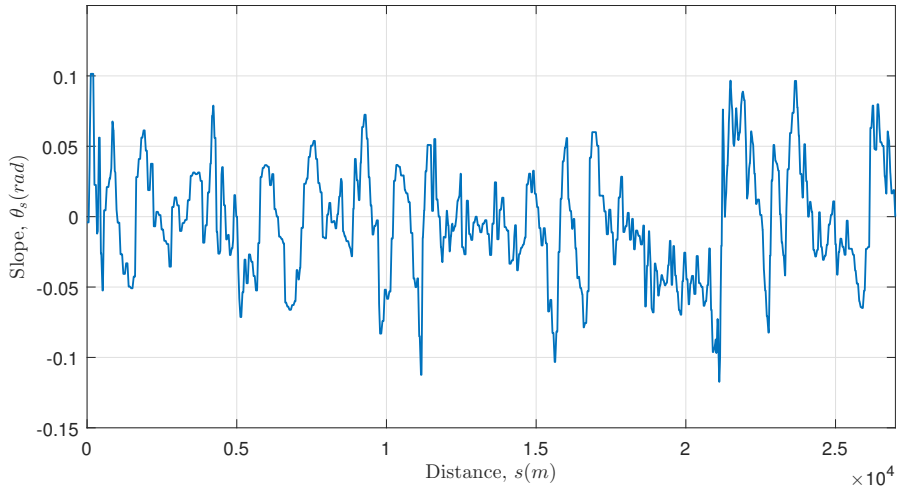

(b) Slope profile.

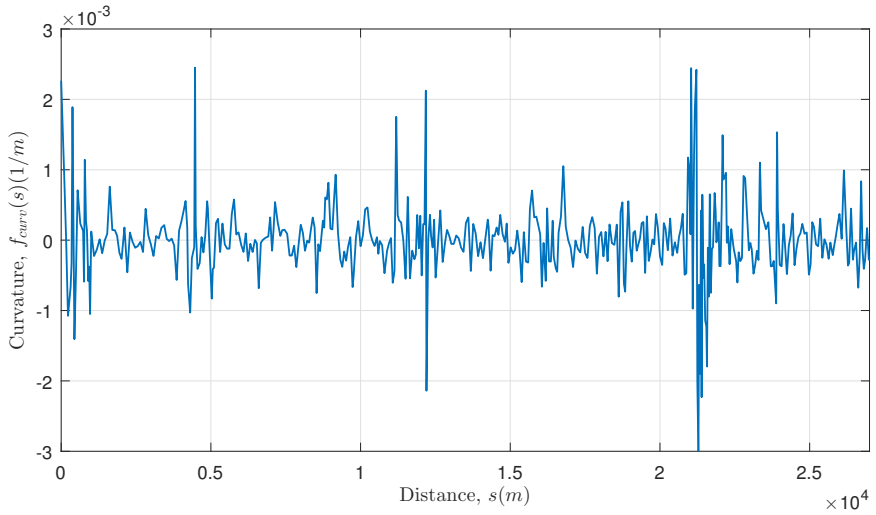

(c) Curvature profile.

Source: Author.

It is possible to notice in Figure 13 that the EDC controller respects the speed limits of the route during the simulation. The predictive action of the EDC controller optimizes the vehicle velocity before entering the speed limit change distance, as shown in Figure 14. Thus, sharp acceleration and braking are avoided, which reduces the fuel consumption and improve the trip comfort for the driver.

The FSC controller on the other hand only adjusts the vehicle velocity after the speed limit setpoint change, which causes an excessive use of acceleration and braking.

Figure 14: Speed limit variation prediction with the EDC controller.

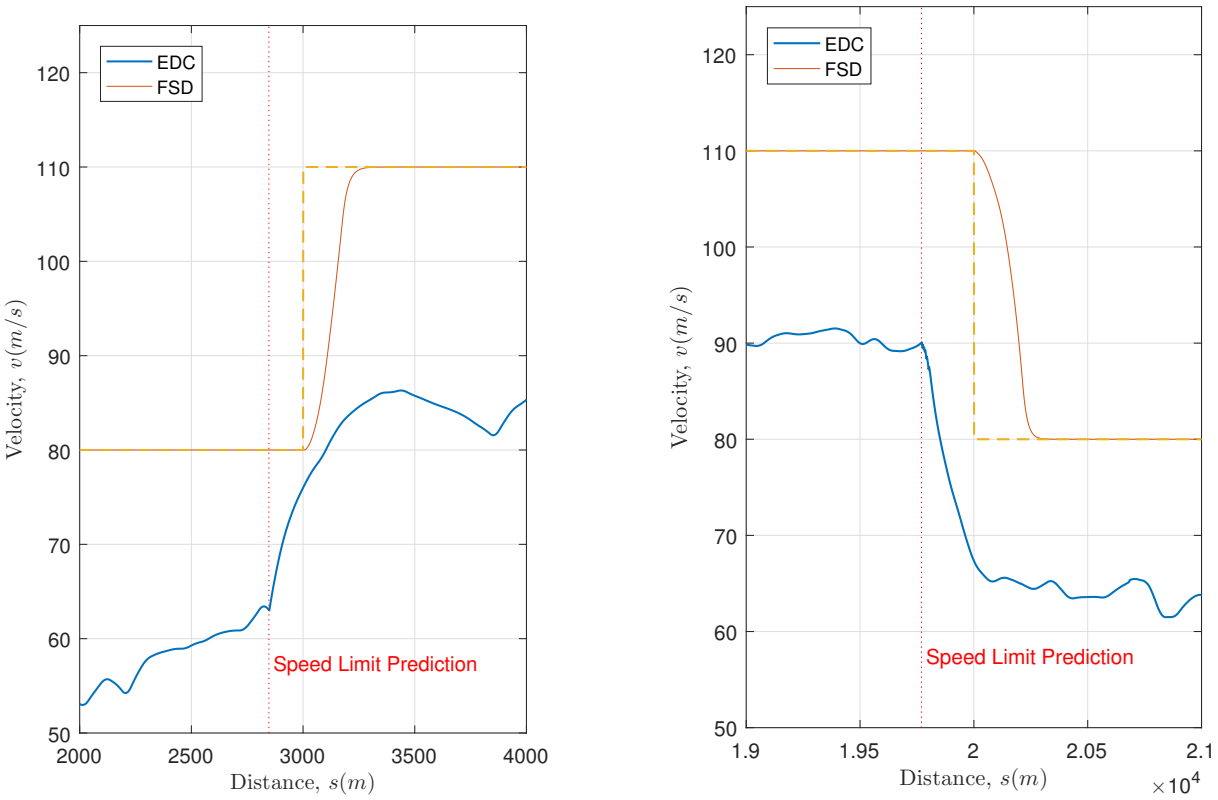

(a) Speed limit raising from 80km/h to 110km/h.

(b) Speed limit reducing from 110km/h to 80km/h.

Source: Author.

Figure 15: Longitudinal and lateral acceleration for the highway scenario.

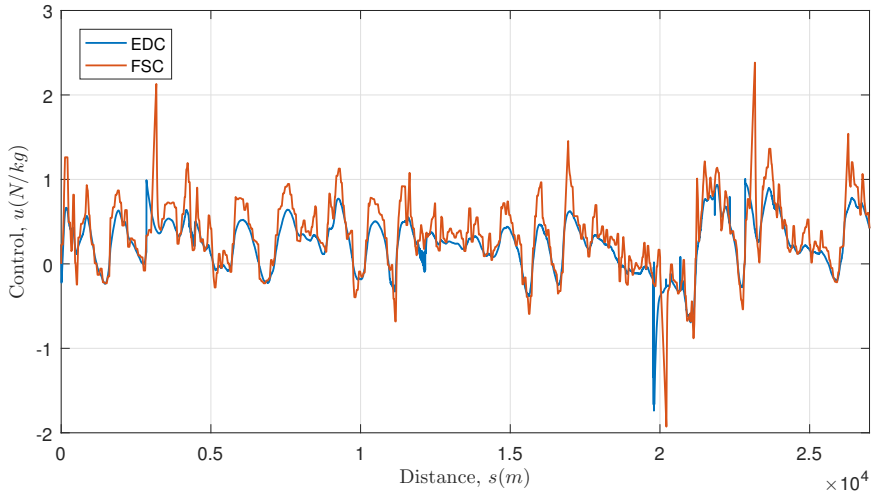

(a) Control input.

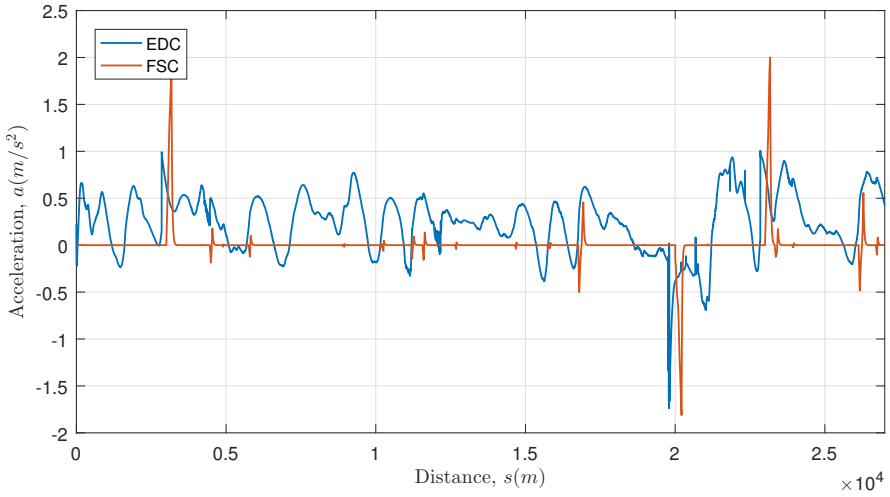

(b) Acceleration performance of the Eco-driving algorithm.

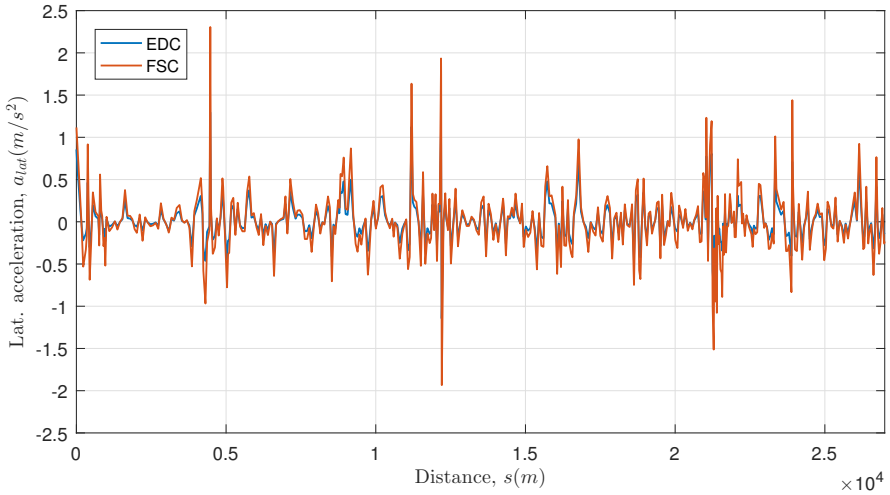

(c) Lateral acceleration.

Source: Author.

The control input for the EDC controller has less variations and a lower amplitude in comparison with the FSD controller, as shown in Figure 15 (a). This has a great impact in the instant fuel consumption of the vehicle. Figure 16(b) shows the total fuel consumption of both vehicles during the trip. It is possible to see that the fuel saving for the EDC controller keeps increasing over the travelled distance. This happens because the EDC controller optimizes the control input using information from the latitude-longitude profile of the route to reduce the tractive force required to maintain the vehicle velocity. The strategies used are to accelerate before an uphill section and use the engine braking in downhill.

Figure 16: Instant and total fuel consumption for the highway scenario.

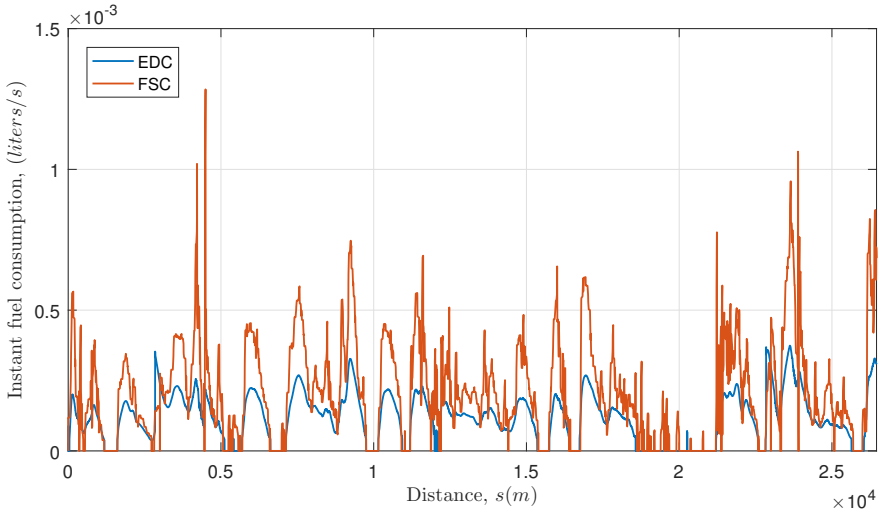

(a) Instant fuel consumption.

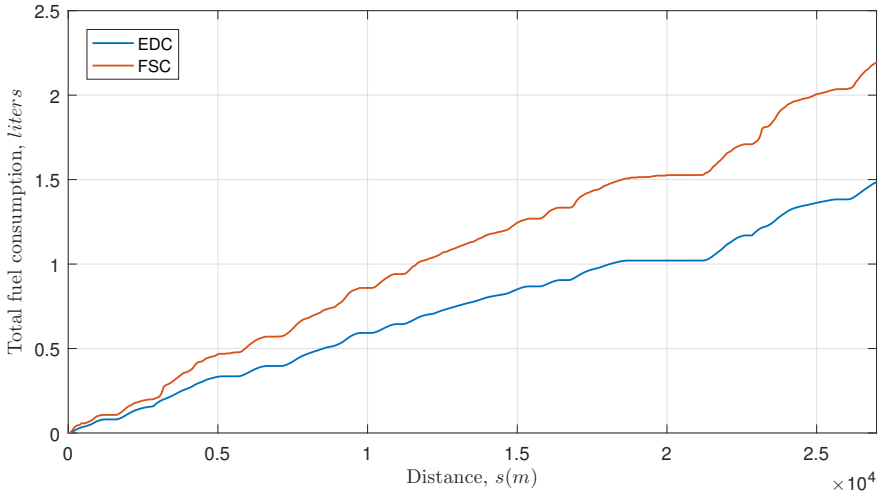

(b) Total fuel consumption.

Source: Author.

Table 4: Comparison of fuel consumption of the two controllers on the highway scenario.

Description	**Controllers**	
	EDC	**FSC**
Trip length	27 km	
Total fuel consumption	1.6590 liters	2.1584 liters
Average fuel consumption	18.18 km/L	12.31 km/L
Elapsed time	20min 50s	16m 49s
Economy of EDC	32.26 %	
Computational time of EDC	9min	

Source: Author.

5.2 Simulation in a city scenario

The second scenario considered for the simulations is a 6km city route from the Campus 2 to Campus 1 of the University of São Paulo at São Carlos. The route map and altitude profile can be seen in Figure 17. There are six different speed limits across the trip: $v_{lim} = 30km/h$ at $s = 0km$, $v_{lim} = 50km/h$ at $s = 800m$, $v_{lim} = 60km/h$ at $s = 1900m$, $v_{lim} = 50km/h$ at $s = 3200m$, $v_{lim} = 60km/h$ at $s = 4700m$, and $v_{lim} = 30km/h$ at $s = 5400m$. Although traffic lights and stop-go situations are not considered in this simulation, the purpose of this test was to evaluate the EDC in a city route, where the curvature profile would have a higher magnitude and the speed limits would be constantly changing. The latitude-longitude data of this route was collected using a GPS with Real Time Kinematic (RTK) correction, with position precision of 0.4cm horizontally and 0.8cm vertically. The results obtained are presented in Figure 18, 20 and 21. Table 5 contain a more detailed results of the simulation. The computational time for the EDC controller calculations is also faster then the simulation time.

Table 5: Comparison of fuel consumption of the two controllers on the city scenario.

Description	**Controllers**	
	EDC	**FSC**
Trip length	6km	
Total fuel consumption	0.360 liters	0.477 liters
Average fuel consumption	15.83km/L	14.55km/L
Elapsed time	13min 58s	11min
Economy of EDC	8.9 %	
Computational time of EDC	6min 8s	

Source: Author.

Figure 17: Simulation city map of São Carlos.

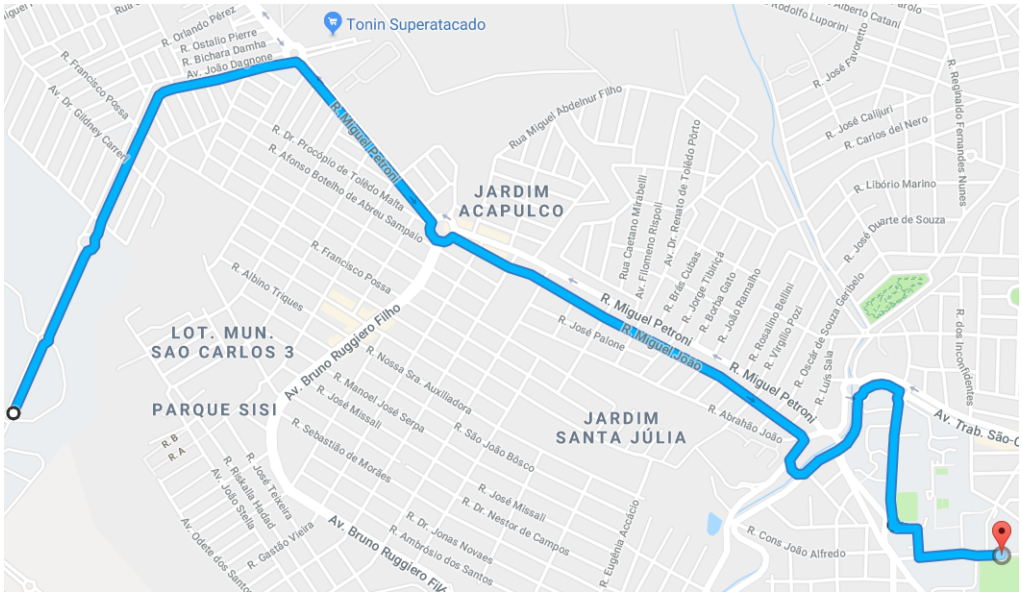

(a) City test map.

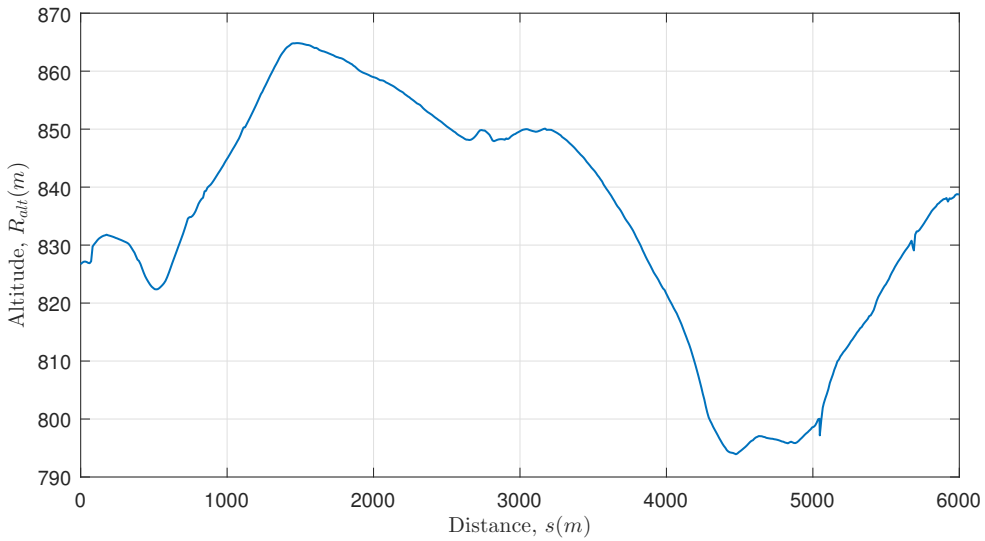

(b) Altitude profile.

Source: Author.

Figure 18: Velocity, slope and curvature profile for the city scenario.

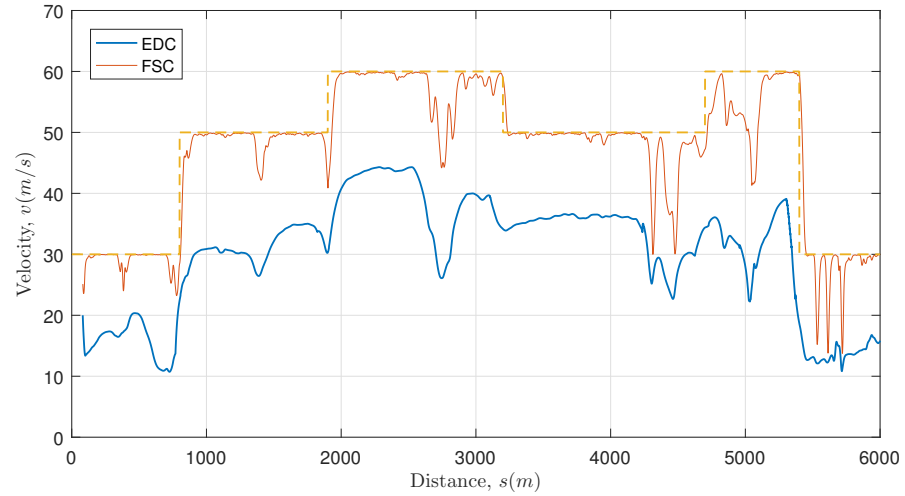

(a) Velocity profile.

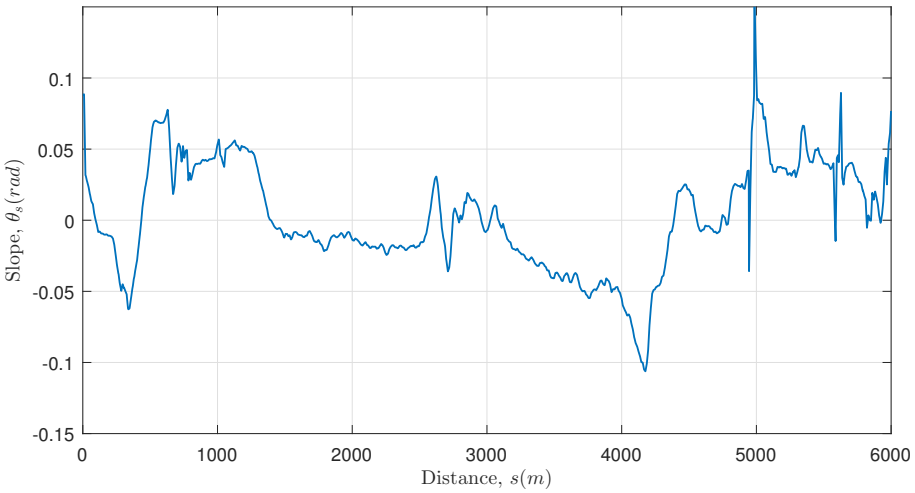

(b) Slope profile.

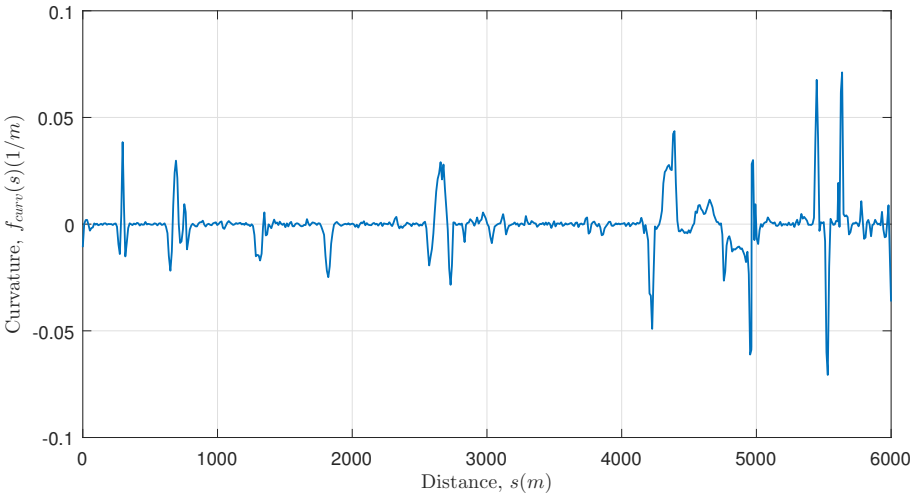

(c) Curvature profile.

Source: Author.

The EDC controller used the predictive action of the NMPC strategy to reduce the velocity of the autonomous vehicle before entering a curve, as shown in Figure 19. This is important to minimize the lateral acceleration affecting the driver, which can increase the discomfort level. Figure 20(c) shows that there is a significant difference in the lateral acceleration for the FSC and the EDC controller.

Figure 19: Road curvature variation prediction with the EDC controller. Velocity is reduced due a constraint in lateral acceleration amplitude before entering the curve.

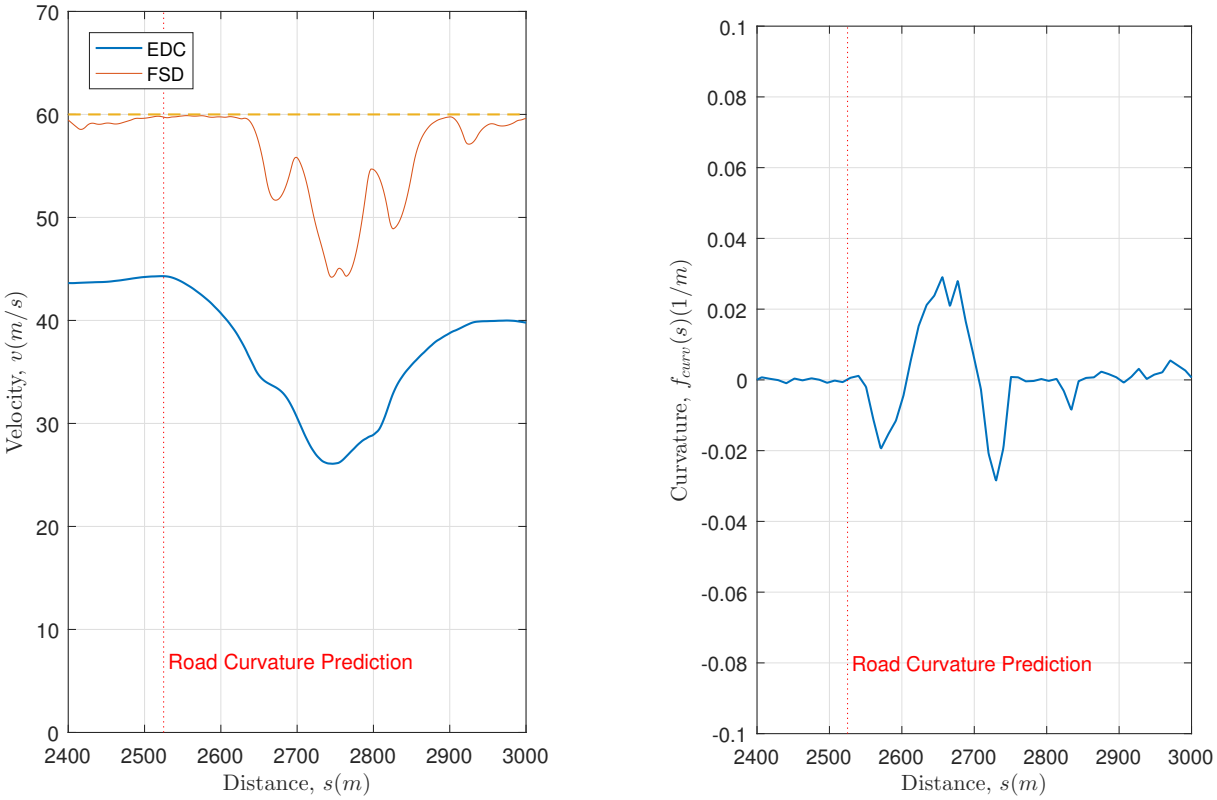

(a) Velocity profile.

(b) Curvature profile.

Source: Author.

Figure 20: Longitudinal and lateral acceleration for the city scenario.

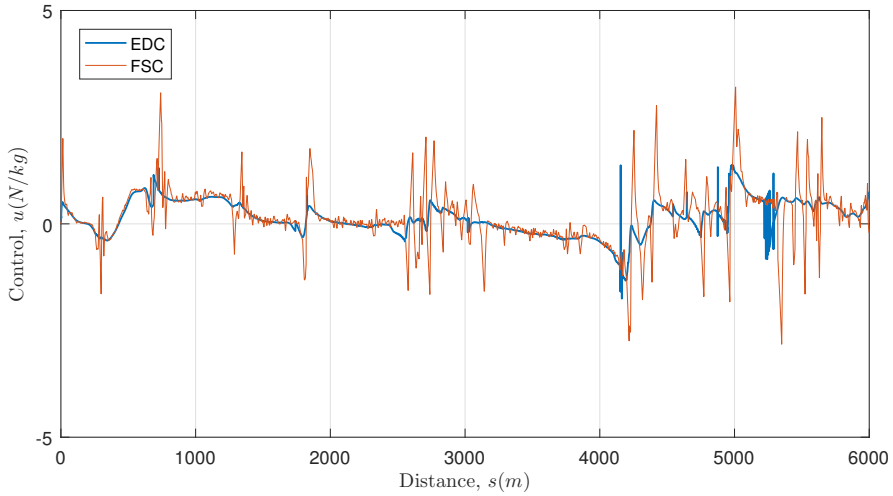

(a) Control input.

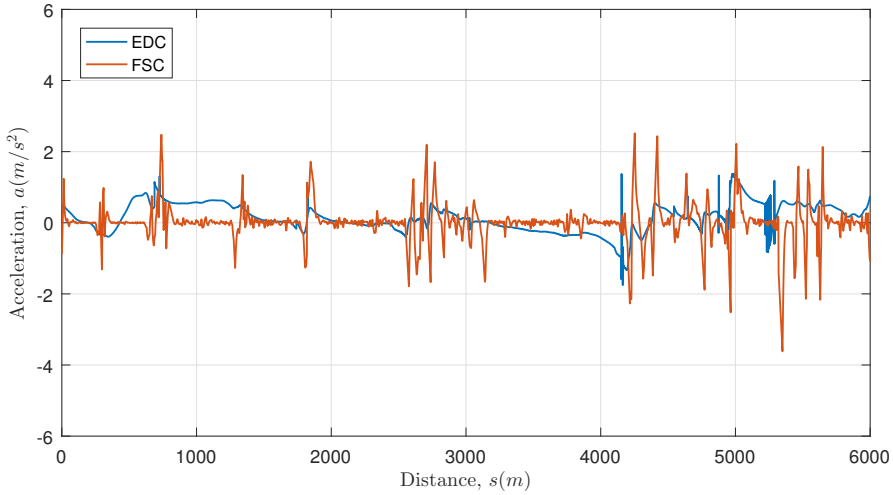

(b) Acceleration performance of the Eco-driving algorithm.

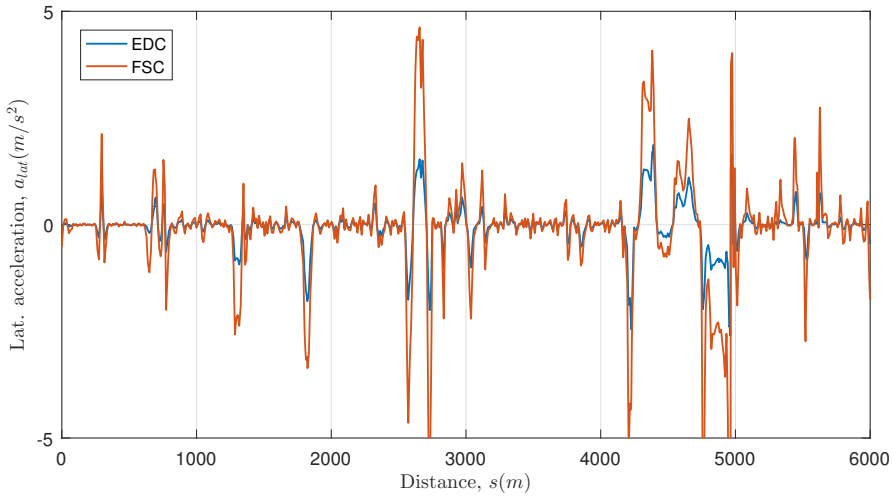

(c) Lateral acceleration.

Source: Author.

Figure 21: Instant and total fuel consumption for the city scenario.

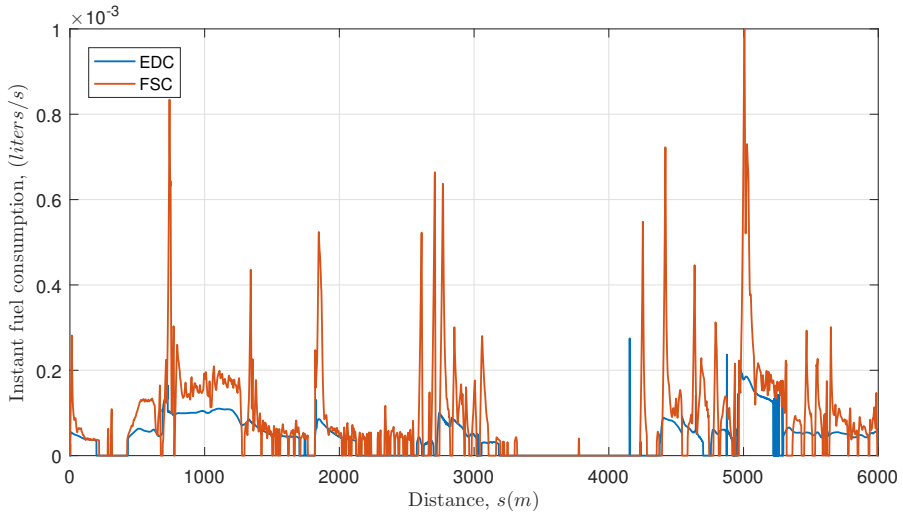

(a) Instant fuel consumption.

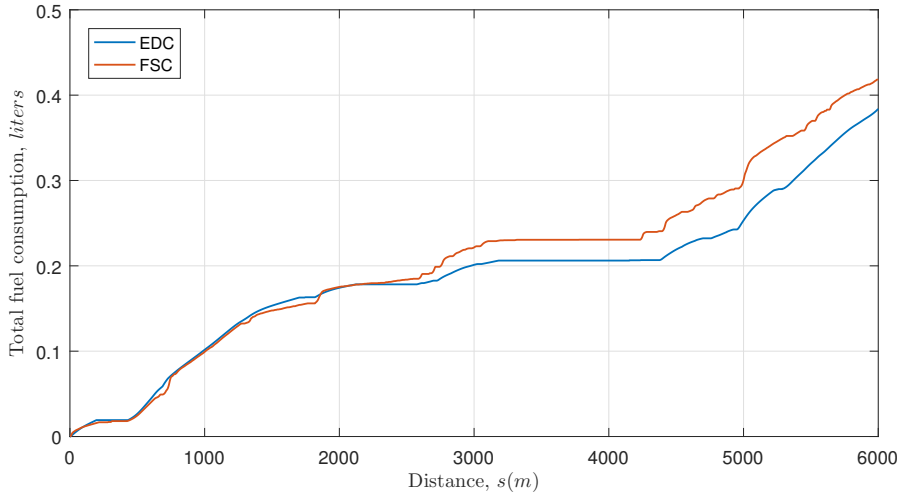

(b) Total fuel consumption.

Source: Author.

The fuel economy of the EDC controller in the city scenario was lower in comparison with the highway scenario. This happened because there were more curves in this route, which made the EDC controller prioritize the comfort level of the driver during the trip. Still, the fuel consumption was reduced during the simulation if compared with the FSC controller.

The instant fuel consumption plot in Figure 21(a) shows how the aggressive driving behavior has a great impact on the fuel consumption of the vehicle, since the sharp acceleration and braking levels are directly associated with the fuel consumption peaks.

6 CONCLUSION

This masters thesis addresses the longitudinal control of an autonomous vehicle, aiming to reduce the fuel consumption and increase safety and a comfort levels. For this purpose, a nonlinear model predictive control system was adopted, in combination with digital road information of the route, which could anticipate the future states of the vehicle and find the optimal solution for the desired objectives. Eco-driving strategies were used as parameters to evaluate the algorithm performance in the NMPC cost function.

A simplified vehicle model proposed by Rakha et al. (2012) is used in this work, since a detailed mathematical description of the vehicle powertrain could increase the computational burden. The state equation of the system describes the acceleration and the velocity of the vehicle over time, based on longitudinal and lateral forces. A decision tree algorithm is trained in combination with field and public vehicle data to estimate the gear selection made by the automatic transmission, which improves the states estimations done by the NMPC algorithm. At last, The VT-CPFM-2 model is used for fuel consumption estimation, since it does not require complex field and laboratory data to be calibrated.

In order to ensure a real time implementation of the proposed Eco-driving algorithm, a fast optimizer method should be adopted. The C/GMRES is used in this work, since it does not use iterative searches to find the optimal solution, as in Newton's method for example. This optimizer is based on a combination of the continuation method, linear equation solver GMRES and forward difference approximations, which proved to be faster than the traditional methods.

The results obtained in the simulations showed that fuel economy can be achieve using the proposed Eco-driving controller, without compromising safety and comfort. In fact, since the acceleration and braking levels are lower than a vehicle with a fixed speed controller, the driver's comfort and safety levels were actually increased. In the highway scenario, the Eco-driving controller could achieve a fuel economy of 32.26% in comparison with the fixed speed controller, without surpass the speed limits of each section. The elapsed time was around 4 minutes longer for the Eco-driving controller, which is acceptable in terms of a highway route.

In the city scenario, the proposed controller could adjust the vehicle velocity according to the streets speed limits and during curves, which are more frequent than in the highway scenario. Also, a fuel economy of 8.97% was achieve, in comparison with the fixed speed controller. In both cases, the Eco-driving strategies adopted were: before a uphill section, increase the vehicle acceleration so the traction power required to maintain the velocity would be reduced; at downhills, use engine braking and let the electronic fuel

injection system cuts fuel consumption to keep the engine running; reduce the magnitude levels of acceleration and braking before and after curves and avoid driving at the speed limit of the route.

For future works, it is suggested the combination of the proposed Eco-driving algorithm with a lateral controller, to adjust the steering and acceleration/braking accordingly. It is also interesting to include the functionalities of and Adaptive Cruise Control, such as adjust vehicle-to-vehicle safe distance.

6.1 Publications

An article was published in Conferência Brasileira de Dinâmica, Controle e Aplicações - DINCON 2017, at São Jose do Rio Preto - SP, titled "Predictive Eco-cruise Control of Autonomous Vehicle Using a Powertrain Model", with the results obtained in this masters thesis.

BIBLIOGRAPHY

ABBAS, M. A. **Non-Linear Model Predictive Control for Autonomous Vehicles**. 2011. Dissertação (Mestrado) — University of Ontario Institute of Technology, 2011.

ABBAS, M. A.; MILMAN, R.; EKLUND, J. M. Obstacle avoidance in real time with nonlinear model predictive control of autonomous vehicles. **Canadian Journal of Electrical and Computer Engineering**, IEEE, v. 40, n. 1, p. 12–22, 2017.

AHSAN, M.; ALIMGEER, K. S. Autonomous ground vehicle. **International Journal of Technology and Research**, Technology and Research Publications, v. 1, n. 3, p. 96, 2013.

ALLGÖWER, F.; FINDEISEN, R.; NAGY, Z. K. Nonlinear model predictive control: From theory to application. **J. Chin. Inst. Chem. Engrs**, v. 35, n. 3, p. 299–315, 2004.

ALRIFAEE, B.; LIU, Y.; ABEL, D. Eco-cruise control using economic model predictive control. In: IEEE. **Control Applications (CCA), 2015 IEEE Conference on**. [S.l.], 2015. p. 1933–1938.

BARKENBUS, J. N. Eco-driving: An overlooked climate change initiative. **Energy Policy**, Elsevier, v. 38, n. 2, p. 762–769, 2010.

BARTH, M.; BORIBOONSOMSIN, K. Energy and emissions impacts of a freeway-based dynamic eco-driving system. **Transportation Research Part D: Transport and Environment**, Elsevier, v. 14, n. 6, p. 400–410, 2009.

BEN-CHAIM, M.; SHMERLING, E.; KUPERMAN, A. Analytic modeling of vehicle fuel consumption. **Energies**, Multidisciplinary Digital Publishing Institute, v. 6, n. 1, p. 117–127, 2013.

CAMACHO, E. F.; BORDONS, C. A. **Model predictive control**. [S.l.]: Springer Science & Business Media, 1999.

CARRESE, S.; GEMMA, A.; SPADA, S. L. Impacts of driving behaviours, slope and vehicle load factor on bus fuel consumption and emissions: a real case study in the city of rome. **Procedia-Social and Behavioral Sciences**, Elsevier, v. 87, p. 211–221, 2013.

CARVALHO, A.; GAO, Y.; GRAY, A.; TSENG, H. E.; BORRELLI, F. Predictive control of an autonomous ground vehicle using an iterative linearization approach. In: IEEE. **Intelligent Transportation Systems-(ITSC), 2013 16th International IEEE Conference on**. [S.l.], 2013. p. 2335–2340.

DIEHL, M.; FERREAU, H. J.; HAVERBEKE, N. Efficient numerical methods for nonlinear mpc and moving horizon estimation. In: **Nonlinear model predictive control**. [S.l.]: Springer, 2009. p. 391–417.

DU, X.; HTET, K. K. K.; TAN, K. K. Development of a genetic-algorithm-based nonlinear model predictive control scheme on velocity and steering of autonomous vehicles. **IEEE Transactions on Industrial Electronics**, IEEE, v. 63, n. 11, p. 6970–6977, 2016.

ECKHOFF, D.; HALMOS, B.; GERMAN, R. Potentials and limitations of green light optimal speed advisory systems. In: IEEE. **Vehicular Networking Conference (VNC), 2013 IEEE**. [S.l.], 2013. p. 103–110.

FALCONE, P.; BORRELLI, F.; TSENG, H. E.; ASGARI, J.; HROVAT, D. A hierarchical model predictive control framework for autonomous ground vehicles. In: IEEE. **2008 American Control Conference**. [S.l.], 2008. p. 3719–3724.

FALCONE, P.; TUFO, M.; BORRELLI, F.; ASGARI, J.; TSENG, H. E. A linear time varying model predictive control approach to the integrated vehicle dynamics control problem in autonomous systems. In: IEEE. **Decision and Control, 2007 46th IEEE Conference on**. [S.l.], 2007. p. 2980–2985.

GRÜNE, L.; PANNEK, J. **Nonlinear model predictive control**. [S.l.]: Springer, 2011.

INSIGHTS, C. **Corporations Working On Autonomous Vehicles**. [S.l.]: Verfügbar unter https://www. cbinsights. com/blog/autonomous-driverless-vehicles-corporations-list, 2016.

JEFFREYS, I.; GRAVES, G.; ROTH, M. Evaluation of eco-driving training for vehicle fuel use and emission reduction: A case study in australia. **Transportation Research Part D: Transport and Environment**, Elsevier, 2016.

JI, J.; KHAJEPOUR, A.; MELEK, W. W.; HUANG, Y. Path planning and tracking for vehicle collision avoidance based on model predictive control with multiconstraints. **IEEE Transactions on Vehicular Technology**, IEEE, v. 66, n. 2, p. 952–964, 2017.

JO, K.; KIM, J.; KIM, D.; JANG, C.; SUNWOO, M. Development of autonomous car—part i: Distributed system architecture and development process. **IEEE Transactions on Industrial Electronics**, IEEE, v. 61, n. 12, p. 7131–7140, 2014.

JUNELL, J.; TUMER, K. Robust predictive cruise control for commercial vehicles. **International Journal of General Systems**, Taylor & Francis, v. 42, n. 7, p. 776–792, 2013.

KAMAL, M. A. S.; MUKAI, M.; MURATA, J.; KAWABE, T. Ecological vehicle control on roads with up-down slopes. **IEEE Transactions on Intelligent Transportation Systems**, IEEE, v. 12, n. 3, p. 783–794, 2011.

_____. Model predictive control of vehicles on urban roads for improved fuel economy. **IEEE Transactions on Control Systems Technology**, IEEE, v. 21, n. 3, p. 831–841, 2013.

KIM, E.; KIM, J.; SUNWOO, M. Model predictive control strategy for smooth path tracking of autonomous vehicles with steering actuator dynamics. **International Journal of Automotive Technology**, Springer, v. 15, n. 7, p. 1155–1164, 2014.

KRASCHL-HIRSCHMANN, K.; FELLENDORF, M. Estimating energy consumption for routing algorithms. In: IEEE. **Intelligent Vehicles Symposium (IV), 2012 IEEE**. [S.l.], 2012. p. 258–263.

LIMA, P. F.; TRINCAVELLI, M.; MÅRTENSSON, J.; WAHLBERG, B. Clothoid-based model predictive control for autonomous driving. In: IEEE. **Control Conference (ECC), 2015 European**. [S.l.], 2015. p. 2983–2990.

LUETTEL, T.; HIMMELSBACH, M.; WUENSCHE, H.-J. Autonomous ground vehicles—concepts and a path to the future. **Proceedings of the IEEE**, IEEE, v. 100, n. Special Centennial Issue, p. 1831–1839, 2012.

MACIEJOWSKI, J. M. **Predictive control: with constraints**. [S.l.]: Pearson education, 2002.

MAYNE, D. Q.; RAWLINGS, J. B.; RAO, C. V.; SCOKAERT, P. O. Constrained model predictive control: Stability and optimality. **Automatica**, Elsevier, v. 36, n. 6, p. 789–814, 2000.

MERSKY, A. C.; SAMARAS, C. Fuel economy testing of autonomous vehicles. **Transportation Research Part C: Emerging Technologies**, Elsevier, v. 65, p. 31–48, 2016.

OHTSUKA, T. A continuation/gmres method for fast computation of nonlinear receding horizon control. **Automatica**, Elsevier, v. 40, n. 4, p. 563–574, 2004.

OZATAY, E.; OZGUNER, U.; FILEV, D.; MICHELINI, J. Analytical and numerical solutions for energy minimization of road vehicles with the existence of multiple traffic lights. In: IEEE. **Decision and Control (CDC), 2013 IEEE 52nd Annual Conference on**. [S.l.], 2013. p. 7137–7142.

OZGUNER, U.; ACARMAN, T.; REDMILL, K. **Autonomous ground vehicles**. [S.l.]: Artech House, 2011.

RAFFO, G. V.; GOMES, G. K.; NORMEY-RICO, J. E.; KELBER, C. R.; BECKER, L. B. A predictive controller for autonomous vehicle path tracking. **IEEE transactions on intelligent transportation systems**, IEEE, v. 10, n. 1, p. 92–102, 2009.

RAKHA, H. A.; AHN, K.; FARIS, W.; MORAN, K. S. Simple vehicle powertrain model for modeling intelligent vehicle applications. **IEEE transactions on intelligent transportation systems**, IEEE, v. 13, n. 2, p. 770–780, 2012.

RAKHA, H. A.; AHN, K.; MORAN, K.; SAERENS, B.; BULCK, E. Van den. Virginia tech comprehensive power-based fuel consumption model: Model development and testing. **Transportation Research Part D: Transport and Environment**, Elsevier, v. 16, n. 7, p. 492–503, 2011.

ROSSITER, J. A. **Model-based predictive control: a practical approach**. [S.l.]: CRC press, 2003.

SAERENS, B. Optimal control based eco-driving. **Leuven, Diss**, 2012.

SAJADI-ALAMDARI, S. A.; VOOS, H.; DAROUACH, M. Nonlinear model predictive extended eco-cruise control for battery electric vehicles. In: IEEE. **Control and Automation (MED), 2016 24th Mediterranean Conference on**. [S.l.], 2016. p. 467–472.

SCHMITT, W. F. **Metodologia de Avaliação de Eficiência Energética em Veículos Leves e seus Impactos em Termos de Uso de Combustíveis**. 2010. Tese (Doutorado) — Universidade Federal do Rio de Janeiro, 2010.

U.S. Environmental Protection Agency. 2015. Disponível em: <<https://www.fueleconomy.gov/feg/atv.shtml>>.

VAEZIPOUR, A.; RAKOTONIRAINY, A.; HAWORTH, N. Reviewing in-vehicle systems to improve fuel efficiency and road safety. **Procedia Manufacturing**, Elsevier, v. 3, p. 3192–3199, 2015.

VAJEDI, M.; AZAD, N. L. Ecological adaptive cruise controller for plug-in hybrid electric vehicles using nonlinear model predictive control. **IEEE Transactions on Intelligent Transportation Systems**, IEEE, v. 17, n. 1, p. 113–122, 2016.

WONG, J. Y. **Theory of ground vehicles**. [S.l.]: John Wiley & Sons, 2001.

YAO, E.; SONG, Y. Study on eco-route planning algorithm and environmental impact assessment. **Journal of Intelligent Transportation Systems**, Taylor & Francis, v. 17, n. 1, p. 42–53, 2013.

YOON, Y.; SHIN, J.; KIM, H. J.; PARK, Y.; SASTRY, S. Model-predictive active steering and obstacle avoidance for autonomous ground vehicles. **Control Engineering Practice**, Elsevier, v. 17, n. 7, p. 741–750, 2009.

ZHANG, K.; SPRINKLE, J.; SANFELICE, R. G. Computationally aware control of autonomous vehicles: a hybrid model predictive control approach. **Autonomous Robots**, Springer, v. 39, n. 4, p. 503–517, 2015.

ZHOU, M.; JIN, H.; WANG, W. A review of vehicle fuel consumption models to evaluate eco-driving and eco-routing. **Transportation Research Part D: Transport and Environment**, Elsevier, v. 49, p. 203–218, 2016.

ZHOU, X.; HUANG, J.; LV, W.; LI, D. Fuel consumption estimates based on driving pattern recognition. In: IEEE. **Green Computing and Communications (GreenCom), 2013 IEEE and Internet of Things (iThings/CPSCom), IEEE International Conference on and IEEE Cyber, Physical and Social Computing**. [S.l.], 2013. p. 496–503.